University of Szeged
Albert Szent-Györgyi Clinical Center, Faculty of Medicine
Department of Neurology

USEFULNESS OF THE LINEAR AND NONLINEAR QUANTITATIVE EEG METHODS IN FUNCTIONAL ANALYSIS OF THE HUMAN BRAIN

Ph.D. Thesis

Anett Járdánházy, M.D.

Supervisor: János Tajti, M.D., PhD.
Associate Professor
Department of Neurology

2008

List of publications providing the basis of this thesis

I. Járdánházy, A. and Járdánházy, T. *Non-linear quantitative electroencephalographic (qEEG) changes during processing of chemo-sensory stimulations: A preliminary study.* Behavioural Brain Research 2008, 194:162-168.

IF : 2.626.

II. Járdánházy, A., Járdánházy, T. and Kálmán, J. *Sodium lactate differently alters relative EEG power and functional connectivity in Alzheimer's disease patients' brain regions*. European Journal of Neurology 2008, 15:150-155.

IF: 2.580.

Abbrevations

AD	Alzheimer’s disease
ADRDA	Alzheimer's Disease and Related Disorders Association
Ag/AgCl	silver/silver chloride
ApoE	Apolipoprotein E
AR	autoregressive
CAP	cyclic alternating pattern
ch	chanel
CNS	central nervous system
CSA	compressed spectral arrays
DSM-IV	Diagnosic and Statistical Manual of Mental Disorders
ECG	electrocardiography
EEG	electroencephalography
EMG	electromyography
ENG	electroneurography
ERP	event-related potencial
ESES	electrical status epilepticus during slow-wave sleep
FDR	false discovery rate
FFT	Fast Fourier Transformation
FIRDA	frontal intermittent rhythmic delta activity
fMRI	functional magnetic resonance imaging
GSW	generalized spike-and-wave
HMPAO	Hexamethylpropyleneamine Oxime
Hz	hertz
ICD-10	International Classification of Disease

ID number	identification number
log	logarithmic
min	minute
MMSE	Mini-Mental State Examination
NINCDS	National Institute of Neurological and Communicative Disorders and Stroke
NLCP	non-linear cross prediction
PD2i	point correlation dimension
PDA	polymorphic delta activity
PET	Positron Emission Tomography
Pi	data points
rCBF	regional cerebral blood flow
REM	rapid eye movement
s	second
SD	standard deviation
SL	synchronization likelihood
SPECT	Single Photon Emission Computed Tomography
SSP	subacute sclerosing panencephalitis
λ	tau

CONTENTS

1. Introduction

1.1 Methods for the functional analysis of the central nervous system

The adaptive reaction of the living organs to the ever changing environment is their most important function. For this purpose they collect external as well as internal information, process it and perform the appropriate action best suiting their needs. There is a machinery organized around this task called nervous system which consist of a central and peripheral parts in the simple and complex animal as well as human organisms. The functions of the nervous system could be studied by the direct observation of the spontaneous or provoked behavior elicited by special stimulation. On the basis of these observations the researchers can construct a 'black box' with appropriate input and output variables. However, they could be interested in the function of these 'black boxes' and make assumptions on their possible structure and related functioning.

There are several disciplines to test these alternative models. The neurophysiologic approaches extend the possibilities of the direct observation giving measurable physical parameters on the event under study. The function of the neurons and glia cells is related to trans-membrane ionic movements which could generate potential and current changes suitable for physical detection and registration. The morphological approaches give information on the structural changes in several stages of the processing mainly with fine space but large time resolution. Some new imaging methods can combine the functional, structural and neuro-biochemical features using isotop radio-ligands (SPECT, PET) or the changes of the nuclear magnetic correlates of the excitable tissue during their work (fMRI) in smaller time scale.

The neurophysiological methods can give high time (in ms range) and because of their mainly indirect character lower space resolution. Several methods are available in experimental and even clinical use for function testing of the central and peripheral nervous system: electromyography (EMG) for muscle and nerve, electroneurography (ENG) for nerve, event-related potential studies (ERP) for peripheral and central sensory as well as motor, electro- and magneto-encephalography (EEG, MEG) for central sensory and motor analysis. The neurophysiological methods are based on the principle that during the work of the excitable tissue there are ion current changes through their membranes which are reflected in measurable electrical current flow and potential differences. These electrical dipoles could be measured by micro-electrodes in situ or after their summation in the surrounding space by electrical macro-electrodes and by detecting the very subtle concomitant magnetic field

changes. Because of the electrical nature of the detection and registration the neurophysiology is often referred as electrophysiology.

The electroencephalography (EEG) first used by Caton (1875) in animal and Berger (1924) in human examinations deals with the electrical phenomena connected to the work of the brain. There are two approaches in the detection of the function of the central nervous system (CNS). In the case of the evoked potentials the examiner is interested in the localized changes of the CNS mainly after sensory stimulations. These localized potential changes are of very small amplitudes therefore they could not be seen in the background EEG activity of comparable size. After using repetitive stimulation and time locked averaging of the recordings the event related component of these potentials became visible and the background activity disappeared. By the help of this technique the integrity of the sensory pathways and the primary data processing of the CNS could be detected. There are, however, situations when the features of the background activity are of more importance than the evoked potential changes. The source of the EEG is thought to be (Niedermeyer, Lopes da Silva) the summation of the postsynaptic dendritic field potentials of the neurons localized near the surface of the cerebral cortex. So it can mainly reflect the influences coming to the site of the recording and only additionally the output reactions through possible returning collaterals. The first analysis of the background EEG signals was made by visual assessment of the recordings. Beside the recognition of abnormal waves the amplitude, frequency of the activity at different sites of the scalp made the basis for the visual as well as instrumental assessment. The changes in the frequency and amplitude content as well as in the local and inter-local organization of the EEG activity were found useful in the characterization of physiological and pathological processes. Different patterns of electrical impulses can indicate various problems in the brain. The sensitivity of the EEG is very high, but the specificity is low. There are only some diseases, where EEG is enough for the diagnosis: for example hypsarrhythmia in West syndrome; Radermacker complex in subacute sclerosing panencephalitis (SSP); generalized spike-and-wave (GSW) discharges in absence epilepsy; triangular waves in hepatic encephalopathy; and specific EEG abnormalities in Jakob-Creutzfeld-syndrom (Rajna, 2006).

The first tools of the instrumental analysis were the analogous frequency analyzers which used filters and integrators for the calculation of the first ‘power spectra’ with low resolution. Later, in the era of digital data processing the autocorrelation function of the EEG or the EEG itself became the basis for the construction of higher resolution power spectra by Fast Fourier Transformation (FFT). The calculation of the cross spectra made possible the

linear interdependence i.e. coherence estimation. Some years ago it became clear that the linear approach alone in the analysis was not enough to get all of information inherent in the EEG signal because of the nonlinearities found in the brain's electrical activity. A dynamical system is linear if all the equations describing its dynamics are linear; otherwise it is nonlinear. In a linear system there is a linear relation between causes and effects (small causes have small effects); in a nonlinear system this is not necessarily so (Stam, 2005). Especially the characterization of the local and global dynamics in the EEG activity needed the use of the combination of linear and nonlinear analysis methods.

1.1.1 Linear neurophysiological methods - spectral analysis in the EEG

There are some basic features of the EEG which are always taken into account in the investigation of the electro-genesis of the brain in physiological and pathological conditions. Even the visual examiner has to make observation on the frequency content of the EEG sample under study. The dominant frequency means that the waves of this particular frequency are seen most frequently in the sample with remarkable amplitude values. Besides the range of the visible frequencies (the lowest and highest detectable) as well as the regularity and organization of the activity have to be recognized. The first two features i.e. dominant and associated frequencies could be detected by the several frequency analysis methods.

Fourier (1807) made the observation that every periodic-like function could be generated by addition of several periodic sines and cosines functions of different frequencies and amplitudes. So the principle of the inverse process which is called Fourier Transformation was to decompose the time-varying signal into periodic waves of different frequencies and amplitudes by assigning amplitude values to every frequency component measured. The first instrumental analyzers worked on analogous principle. The frequencies were selected by a set of analogous filters and the area below the curves was measured by integrator circuits for getting amplitude values in the given particular frequency range defined by the filter characteristics. Based on the technical possibilities the selection of the traditional frequency bands (alpha, beta, theta, delta and gamma) was enough correct for the examinations at that time. By the advent of the digital data processing the so called periodograms were used first for spectral calculations. On the basis of the distance between two consecutive zero crossing or wave peaks these methods separated the EEG waves and summarized the amplitude values in the selected range to show the frequency and amplitude relations.

Secondly an indirect calculation was used for the estimation of the frequency-amplitude functions called power spectra. The auto-correlograms which give the measure of the dependence of the differently shifted values of the original signal were estimated first. Later these correlograms were Fourier transformed to go from time to frequency domain to get finally power spectra. In a more advanced method the power spectra were calculated directly from the samples of fixed length (where $N=2^n$) using a simplified quick algorithm called Fast Fourier Transformation.

The digitalization itself and the use of the digital transformations, however, need to fulfill strict assumptions what are only seldom met. The assumption of the infinite length and stationarity of the epochs are the most important points among them. The resulting lower resolution and the wider confidence interval around the calculated power spectra decrease their reliability and usefulness. The power spectra calculated on the basis of the autoregressive (AR) models fitted to the EEG samples are better for the comparison of the consecutive epochs because of their narrower confidence intervals based on their higher level of freedom. The fitted AR models of different order (n) give the coefficient of the function for the estimation of the next point from the values of previous n points of the EEG curve. These methods could give information on the frequency-amplitude content of the electrical activity of a scalp electrode in the multi-electrode montage. The inter-electrode relations in frequency domain could be estimated by the so called coherence calculation which is based on the use of the cross-spectra.

The whole power spectra were used only in some applications e.g. in the visual trend analysis of the compressed spectral arrays (CSA) at the intensive care units. Relative and absolute band powers were compared instead in the majority of the studies. Here are some recent investigations as follows: Otto (2008) has used EEG spectral analysis for narcosis monitoring in animal experiments. The cognitive decline (van der Hiele et al., 2007) and mental functions of the early Alzheimer's patients (Czigler et al., 2008) were correlated by the EEG's spectral and complexity features. Spectral EEG and coherence changes were investigated after performance test in the AD (Hidasi et al., 2007) The spectral changes were found to reflect the complexity of the cognitive tasks (Kurova and Cheremushkin, 2007). Besides some other parameters were derived from the spectra to highlight and extract the specific information inherent in the EEG signal at various conditions. The dominant frequency is represented by a visible peak in the spectra, the mean or median frequency in a given frequency band are calculated characteristic values not always seen clearly. The spectral edge-95 is a frequency value above it only the 5 percent of the total power could be found.

The robust derived Hjorth's parameters: Activity, Mobility and Complexity gave a purposeful characterization of the different physiological and pathological conditions. These linear methods were and even are the most popular in the quantitative EEG because of their robustness and relative easy interpretation.

1.1.2. Nonlinear dynamical analysis of EEG

1.1.2.1. Short historical background

The beginning of the nonlinear EEG analysis was in 1985, when Rapp et al. described their results with 'chaos analysis' of spontaneous neural activity in the motor cortex of a monkey (Rapp et al., 1985), and Babloyantz et al. published the correlation dimension of human sleep EEG (Babloyantz et al., 1985). 'Deterministic chaos' is a paradoxical phenomenon, because it describes unpredictable behaviour in deterministic dynamical systems (Li and Yorke, 1975).

Edward Lorenz published the first graph of a strange attractor, the so-called 'Lorenz attractor' (Lorenz, 1963). Packard et al. transformed a time series of observations into a representation of the dynamics of the system in a multi-dimensional state space or phase space (Packard et al., 1980). In 1983, Grassberger and Procaccia described, how to calculate the correlation dimension of a reconstructed attractor (Grassberger and Procaccia, 1983a, b). In the early phase of nonlinear EEG analysis the aim was to search for low-dimensional chaotic dynamics in various types of EEG. Later with the 'surrogate data testing' the check of the validity of the results became possible. Now the new measures of the EEG are based upon phase synchronization and generalized synchronization.

There are so much nonlinear methods, for example nonlinear forecasting, cross recurrence, false nearest neighbors, cross prediction, but here I would like to introduce some of the most important nonlinear time series methods:

1. Nonlinear cross prediction
2. Phase synchronization
3. Mutual dimension
4. Correlation dimension
5. Synchronization likelihood

1.1.2.2. Nonlinear cross prediction

This method is based on nonlinear forecasting and the predictability of a time series and its time reversed copy (Stam et al., 1998). Here we have to choose a point on the attractor, and to predict the future course of this point by fitting a local linear model to the dynamics. This method is suitable for detection of amplitude and time asymmetry (Stam et al., 1998), and for test irreversibility based upon symbolic dynamics (Daw et al., 2000). Nonlinear cross prediction (NLCP) is seemed to be useful in various areas of physics: for the sleep analysis of healthy adults, children with epilepsy, premature and full-term newborns. It was found that the NLCP test provided evidences of significant non-linear dynamics in all epochs of non-REM sleep, when electrical status epilepticus during slow-wave sleep (ESES) was evident. Only during this stage, the possible presence of low-dimensional chaos could also be suspected. EEG without ESES could not be distinguished from linearly filtered noise (Ferri et al., 2001). Sleep EEG tends to show non-linear structure only during cyclic alternating pattern (CAP) periods, both during S2 and SWS. During CAP periods, non-linearity can only be detected during the phase A1 subtypes (and partially A2) of CAP. The A3 phases show characteristics of non-stacionarity and bear some resemblance to wakefulness (Ferri et al., 2002). The structure of sleep EEG in newborns is significantly different from that of adults, it cannot be distinguished from that of high-dimensional noise in the majority of epochs, and shows a tendency to become nonlinear in nature, mostly during quiet sleep in a small percentage of the epochs analyzed (Ferri et al., 2003). Another study investigated that frontal intermittent rhythmic delta activity (FIRDA) was more predictable than polimorphic delta activity (PDA). Most PDA segments could not be distinguished from linearly filtered noise. In contrast, FIRDA activity showed strong evidence of nonlinear dynamics (Stam and Pritchard, 1999).

1.1.2.3. Phase synchronization

‘Synchronization of chaos refers to a process, wherein two (or many) systems (either equivalent or nonequivalent) adjust a given property of their motion to a common behavior due to a coupling or to a forcing (periodical or noisy)’ (Boccaletti et al., 2002). Phase synchronization is characterized by a non uniform scattering of the phase differences between two time series, and it can be computed using the Hilbert transform (Mormann et al., 2000; Tass et al., 1998) or by means of wavelets analysis (Lachaux et al., 1999). The difference between the analysis of Mormann et al. and Tass et al. was that Mormann et al. used the circular variance to characterize the distribution of phase differences, while Tass et al. used a Shannon information entropy measure. Further it was found that this method was suitable not

only to detect the direction of coupling between two systems (Cimponeriu et al., 2003; Rosenblum and Pikovsky, 2001; Smirnov and Bezruchko, 2003), but also to track rapid changes in the level of coupling between dynamical systems (Breakspear et al., 2004; Kozma and Freeman, 2002; Van Putten, 2003a, b). Mean phase coherence R─ a bivariate measure for phase synchronization – can be archived with cellular nonlinear networks's using polinomial-type templates (Sowa et al., 2005), this could be promising method for brain-computer interfaces, and it provides a new idea for recognition of mental tasks (Aihua and Yuhan, 2005).

1.1.2.4. Mutual dimension

Mutual dimension is the measure of the shared degrees of freedom of two dynamical systems (Buzug et al., 1994; Meng et al., 2001; Wojcik et al., 2001). This method seemed to be suitable for studying EEG changes during mental activity (Stam et al., 1996; Meyer-Lindenberg et al., 1998; Aftanas et al., 1998). Mutual dimension is sensitive not only to look for subtle aspects of emotional processing (Aftanas et al., 1998), but also to examin EEG changes during simple visual information processing and mental archimetric (Stam et al., 1996).

1.1.2.5. Correlation dimension

Correlation dimension method has been developed to characterize the reconstructed attractor in a quantitative way. Correlation dimension is a useful method in the analysis of different pathological conditions: for example in epilepsy detection (Kannathal et al., 2004a; Adeli et al., 2007; Lee et al., 2007, Járdánházy et al., 2007) and in Alzheimer's disease (Jelles et al., 2008). With this measure, the dynamic and depth levels of anesthesia also can be detected (Gifani et al., 2007; Lalitha and Eswaran, 2007). This method is also suitable for the nonlinear dynamical analysis of the neonatal time series: to find the relationship between neurodevelopment and complexity (Janjarajitt et al., 2008a) and between sleep state and complexity (Janjarajitt et al., 2008b).

The only problem with this method is, that in case of long epochs the biological data of the system has uncontrollably changes (e.g. int he shifts from sleeping to waking, or from quiescence to alertness). Therefore Skinner's laboratory developed the PD2i algorhythm to address data nonstationarity. In nonstationary data, the vectors made from 'points' of data that are stationary with respect to the 'point' that the reference vector is in (a 'point' is a small strip of data, m*τ data points long) will contribute uncontaminated vector-difference lengths

only to the small log *r* part of the scaling region. (The further details of the method can be found in Data analysis section 3.6.2.).

1.1.2.6. Synchronization likelihood

The synchronization likelihood is a measure of the generalized synchronization between two dynamic systems *X* and *Y* (Stam and van Dijk, 2002). This method seemed to be suitable for studying seizures: in the neonatal EEG (Altenburg et al., 2003; Smit et al., 2004); in adult intensive care unit patients (Slooter et al., 2006); in nocturnal frontal lobe (Ferri et al., 2004) and in mesial temporal lobe epilepsy (Ponten et al., 2007). It seemed to be also suitable for the analysis of other brain pathologies: brain tumors (Bartolomei et al., 2006); schizophrenia (Micheloyannis et al., 2006); stroke (Molnár et al., 2006a, b); Alzheimer disease (Stam et al., 2003a; Babiloni et al., 2004; Pijnenburg et al., 2004; Stam et al., 2005; 2007; Járdánházy et al., 2008; Czigler et al., 2008). SL can be used to study the global dynamics in healthy adults (Stam et al., 2002; 2003b; 2004; Smit et al., 2007).

The cognitive mental processes need a lot of connections and cooperation among different specific as well as non-specific areas of the brain. The local and global (i.e. inter-local) organization of the data processing suppose a good metabolic state in the background for the proper functioning. The smell and taste sensations are special types of cognitive processes because of their old phylogenetical and strong emotional character. There are reports on the issue that the disturbancies of the smell and taste sensations are the first and fundamental signs of the mental decline in the dementias.

The Alzheimer's dementia is characterized by localized damage of the neural as well as glial elements with a consequent decrease of the circulation and metabolism in the involved areas. The infusion of the metabolite sodium lactate which was found an effective vasodilator and metabolic enhancer in healthy population seemed to be a potential test treatment in Alzheimer's patients.

These two experimental conditions looks appropriate for the comparison of different linear and non-linear EEG analysis methods reflecting several sides of the metabolic and functional organization.

There is not enough evidence now, however, on the issue what linear and nonlinear studies from the processing battery can give the most useful additional information in the exploration of special cognitive processes and dementia conditions for early diagnosis. Therefore the aim of the present study was to use and compare linear and nonlinear methods in different 'low and high level' reactions of the human brain.

2. Aims

Based on the premises found in the Introduction chapter we decided to get information on the usefulness of the different linear- and nonlinear EEG analysis methods for the selection of appropriate technical tools in the early diagnosis of dementia syndromes.

In the first study, therefore, we wanted to know whether

A) The changes of the local (Point Correlation Dimension (PD2i)) or global/inter-local (Synchronization Likelihood (SL)) organization of the scalp EEG can better characterize the chemo-sensory cognitive process after pleasant smell and taste stimulation in healthy persons.

B) Which parameters are suitable for the proper collection of a normative database for a later comparison with some neurodegenerative diseases?

In the second investigation we tried to answer the question

C) Whether the power spectral analysis can reflect the different alteration of the Alzheimer's brain regions after metabolic active sodium lactate infusion.

D) Can the linear as well as nonlinear inter-local synchronization likelihood analysis add some more information on the metabolic reactivity for the differentiation of the altered brain regions?

3. Materials and methods

3.1. Healthy subjects

Nine healthy subjects (two men, seven women) whose mean age was 49 +-19 years, participated in the first study. None of them had any neurological disease, nor had symptomatic viral infection or used psychoactive medication during the investigation or in the previous weeks. All of them were right handed and non-smokers. All subjects underwent a standard clinical examination, including neurological assessment. Based on their personal reports and our orientational examination made by some smell and taste samples all of them were representative for normosmic and taste population. After the EEG recording, a verbal description of the patients experience concerning the two kinds of stimuli was given. The protocol for this study was approved by the Medical Ethics Committee of the University Hospital. All volunteers signed a written consent to take part in the study.

3.2. Alzheimer's disease patients

Twelve Caucasian AD patients (five men, seven women) with an average age of 72.67 ± 2.57 years participated in the second investigation. All of them met the criteria of the International Classification of Disease (ICD-10) and NINCDS-ADRDA for probable AD. They had moderate-to-severe dementia syndrome as their Mini-Mental State Examination (MMSE) score was 13.4 ± 5.72 points. The probands were late onset AD cases and sporadic type. Standard clinical examination, including neurological assessment, had been performed on each participant. Five patients out of twelve (three female and two men) participated in an earlier study (Kálmán et al., 2005a) where the lactate effect on the regional cerebral blood flow (rCBF) was studied by ^{99m}TC-HMPAO SPECT as well. Their average age was 73.6 ± 2.30 years. (For the reference see the publication's Table 2. with the proband ID number 3, 4, 8, 12, 13 where their ApoE genotype, anxiety symptoms and the localization of the decreased rCBF as well as changes observed after sodium lactate infusion are shown.) The other seven patients (four women and three men, with an average age of 72.1 +-2.71 years) participated only in the EEG studies.

None of the AD probands had a history of panic disorder, agoraphobia with panic attacks or generalized anxiety disorders (according to the DSM-IV and ICD-10 criteria) based on the interview with the patients and their caregivers. No psychotropic medication, e.g., acetylcholinesterase inhibitors, nootropics, anxiolytics, antidepressants or other drugs known to interfere with the EEG, were administered three weeks before or during the experiments.

All AD patients were non-smokers and outpatients. All volunteers and caregivers gave their informed consent to participate. The study protocol was approved by the local Medical Ethics Committee.

3.3. EEG recordings

The EEG was recorded in a silent room with eyes closed. The subjects were seated in a comfortable chair under constant control for their state of alertness. The Ag/AgCl electrodes were placed on the scalp according to the international 10-20 system. EEG signal was recorded (EEG-16X/Mikromed, Hungary; time constant 0.3 s; high frequency filter 70 Hz; common average reference) and after digitalization (256 Hz, 12 bit, with LI-01/A laboratory interface/Mikromed, Hungary, by their Neuromap program) simultaneously stored on hard disk. The records were inspected off-line to remove epochs with movement artifacts, muscle activities, eye blinking and drowsiness.

The analyses were performed on 16 channels (Fp1, Fp2, F3, F4, F7, F8, C3, C4, T3, T4, T5, T6, P3, P4, O1, and O2) (*Fig. 1*).

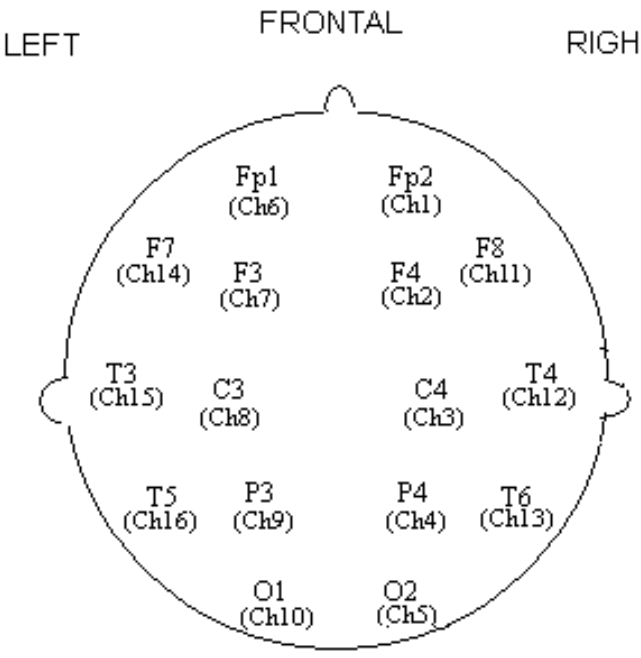

Fig. 1. Topographic view of scalp electrode positions used in our studies.

3.4. Smell and taste stimuli

During the baseline condition (which was 30s) the subjects sat still with closed eyes and no stimuli were applied. This control interval was divided into first and second 15s parts. After 30s, the patients were given a perfume smell continuously for 30s. After an interval of a few minutes of rest with eyes open (which helped the patients keep the arousal level constant) a 30s EEG with closed eyes without activation was recorded again. After this a small piece of milk chocolate was placed near the tip of the subjects' tongue. During this, they continued to sit with eyes closed for 30s to feel the taste. The subjects kept the chocolate near the tip and waited for its taste. After the recordings a pleasant-unpleasant scale was given to the patients.

3.5. Infusion protocol

In the second investigation twenty minutes were given for each Alzheimer's volunteer to adapt to the circumstances to reduce stress levels. After this, 5 mL/kg sodium lactate (0.5 M) was infused over 20 min. The intravenous lines were placed into both forearms of the participants. ECG, blood pressure, venous blood gas and electrolytes were assessed before the study, every 5 min during the infusion and 10 min after the treatment. In order to control any potential side-effect (panic attack, alkalosis, and ECG changes), all parameters were continuously monitored by an intensive care specialist.

3.6. Data analysis

3.6.1. Spectral analysis

The off-line spectral analysis was performed by means of Fast Fourier Transform facility of the DigEEGXP v2.0 program on 16 s long (4096 points) epochs. This program uses 'split-radix ' FFT algorithm for the calculation of the power spectra.

Mathematical background of split –radix FFT algorithm (cited from Duhamel and Vetterli, 1990)

The split-radix FFT is a fast Fourier transform (FFT) algorithm for computing the discrete Fourier transform (DFT). In particular, split radix is a variant of the Cooley-Tukey FFT algorithm that uses a blend of radices 2 and 4: it recursively expresses a DFT of length N in terms of one smaller DFT of length $N/2$ and two smaller DFTs of length $N/4$.

The split-radix FFT, along with its variations, long had the distinction of achieving the lowest published arithmetic operation count (total exact number of required real additions and multiplications) to compute a DFT of power-of-two sizes N. Although the number of

arithmetic operations is not the sole factor in determining the time required to compute a DFT on a computer, the question of the minimum possible count is of important theoretical interest.

Split-radix decomposition

Recall that the DFT is defined by the formula:

$$X_k = \sum_{n=0}^{N-1} x_n \omega_N^{nk}$$

where k is an integer ranging from 0 to $N - 1$ and ω_N denotes the primitive root of unity:

$$\omega_N = e^{-\frac{2\pi i}{N}},$$

and thus $\omega_N^N = 1$.

The split-radix algorithm works by expressing this summation in terms of three smaller summations. Below we give the "decimation in time" version of the split-radix FFT; the dual decimation in frequency version is essentially just the reverse of these steps.

First, a summation over the even indices x_{2n_2}. Second, a summation over the odd indices broken into two pieces: $x_{4n_4+1}$and x_{4n_4+3}, according to whether the index is 1 or 3 modulo 4. Here, n_m denotes an index that runs from 0 to $N / m - 1$. The resulting summations look like:

$$X_k = \sum_{n_2=0}^{N/2-1} x_{2n_2} \omega_{N/2}^{n_2 k} + \omega_N^k \sum_{n_4=0}^{N/4-1} x_{4n_4+1} \omega_{N/4}^{n_4 k} + \omega_N^{3k} \sum_{n_4=0}^{N/4-1} x_{4n_4+3} \omega_{N/4}^{n_4 k}$$

where we have used the fact that $\omega_N^{mnk} = \omega_{N/m}^{nk}$. These three sums correspond to *portions* of radix-2 (size $N/2$) and radix-4 (size $N/4$) Cooley-Tukey steps, respectively. The underlying idea is that the even-index subtransform of radix-2 has no multiplicative factor in front of it, so it should be left as-is, while the odd-index subtransform of radix-2 benefits by combining a second recursive subdivision.

These smaller summations are now exactly DFTs of length $N/2$ and $N/4$, which can be performed recursively and then recombined.

More specifically, let U_k denote the result of the DFT of length $N/2$ (for $k = 0, \ldots, N/2 - 1$), and let Z_k and Z'_k denote the results of the DFTs of length $N/4$ (for $k = 0, \ldots, N/4 - 1$). Then the output X_k is simply:

$$X_k = U_k + \omega_N^k Z_k + \omega_N^{3k} Z'_k.$$

This, however, performs unnecessary calculations, since $k \geq N/4$ turn out to share many calculations with $k < N / 4$. In particular, if we add $N/4$ to k, the size-$N/4$ DFTs are not changed (because they are periodic in k), while the size-$N/2$ DFT is unchanged if we add $N/2$ to k. So, the only things that change are the ω_N^k and ω_N^{3k} terms, known as twiddle factors. Here, we use the identities:

$$\omega_N^{k+N/4} = -i\omega_N^k$$
$$\omega_N^{3(k+N/4)} = i\omega_N^{3k}$$

to finally arrive at:

$$X_k = U_k + \left(\omega_N^k Z_k + \omega_N^{3k} Z'_k\right),$$
$$X_{k+N/2} = U_k - \left(\omega_N^k Z_k + \omega_N^{3k} Z'_k\right),$$
$$X_{k+N/4} = U_{k+N/4} - i\left(\omega_N^k Z_k - \omega_N^{3k} Z'_k\right),$$
$$X_{k+3N/4} = U_{k+N/4} + i\left(\omega_N^k Z_k - \omega_N^{3k} Z'_k\right),$$

which gives all of the outputs X_k if we let k range from 0 to $N / 4 - 1$ in the above four expressions.

Notice that these expressions are arranged so that we need to combine the various DFT outputs by pairs of additions and subtractions, which are known as butterflies. In order to obtain the minimal operation count for this algorithm, one needs to take into account special cases for $k = 0$ where the twiddle factors are unity and for $k = N / 8$ where the twiddle factors are $(\pm 1 - i)/\sqrt{2}$ and can be multiplied more quickly. Multiplications by ± 1 and $\pm i$ are ordinarily counted as free (all negations can be absorbed by converting additions into subtractions or vice versa).

This decomposition is performed recursively when N is a power of two. The base cases of the recursion are N=1, where the DFT is just a copy $X_0 = x_0$, and N=2, where the DFT is an addition $X_0 = x_0 + x_1$ and a subtraction $X_1 = x_0 - x_1$.

These considerations result in a count: $4N\log_2 N - 6N + 8$ real additions and multiplications, for N a power of two greater than 1.

Relative (expressed as percentage of the whole spectrum) EEG power values were calculated and considered for each electrode due to their lower inter-subject variability (Nuwer, 1988). The relative power values were calculated in the delta (0.5-4 Hz), theta (4-8

Hz), alpha (8-12 Hz), beta1 (12-20 Hz) beta2 (20-30 Hz), and gamma (30-48 Hz) frequency bands.

3.6.2. Point correlation dimension

Mathematical background of Point Correlation Dimension (PD2i)

The point correlation is an algorithm that allows compution of the dimension as a function of time (Skinner et al., 1994; 2000; 2002).

In order to be able to quantify the dimensional complexity of a system its state space (phase space) has to be constructed. The coordinates of this space are the degrees of freedom of the analyzed system. It is possible to construct the state space from a single time series (such as the EEG) by the delay-time embedding procedure (Packard et al., 1980; Takens, 1985). Grassberger and Procaccia (1983a, b) developed an algorithm that provides an efficient procedure in the calculation of correlation dimension (D2). Consider the set of {X_i, i=1,….,N}of points on the attractor, i.e., $X_i \equiv X(t+i\tau)$ with a fixed time increment τ between the measurements, then correlation integral is defined as

$$C(m,r,n) = \lim_{N\to\infty}\left[\frac{1}{N^2}\sum_{i=1}^{N}\sum_{\substack{j=1\\ i\neq j}}^{N}\Theta\left(r-\left|X_i - X_j\right|\right)\right]$$

where *m* is the embedded dimension, r is the fixed distance, θ(y) is the Heaviside step function, with θ(y)=1 for y>0 and θ(y)=0 for y≤0, and $\left|X_i - X_j\right|$ shows the distance in any usual norm.

The correlation dimension (D2) of a time-series is defined as

$$C(r,n) = r^{D2}$$

where C(r,n) is the cumulative number of all rank-ordered vector-differences within a range (r) and n is the number of vector-differences. Vector-differences are calculated in the following way: A reference vector (nref) is chosen that begins at a specific point in the data and takes a specified number (*m*) of sequential time-steps in the data stream that are of a fixed length (***τ***). Each value encountered in the time-steps is used as one coordinate of the m-dimensional vector. A different vector is then made by moving to a new starting point, for

example to the next point in the time-series using the same number of τ-steps. Then another vector is made by starting at the third point in the series, and so on for all of the points in the time series. All possible vector-differences for every possible nref made with a given embedding dimension (*m*) are then rank-ordered and a log C (r,n) versus log r plot is made.

The slope of the linear region in this plot is then measured; this linear region reflects the range of r over which the model

$$C(r,n) = \frac{\log C(r,n)}{\log r}$$

is valid. The value of m is incremented and the corresponding slope noted, thus yielding slope and m pairs. The values of *m* are selected to span the size of the expected D2 value (that is, *m* ranges from 1 to 2D2 + 1). The number of embedding dimensions is relevant up to the point where its increment is no longer associated with an increase in slope (i.e., it converges). D2 is defined as the slope of the linear region at the convergent values of *m*.

Mathematical stationarity is presumed in the above application which presumption is rarely tenable for biological data. The „pointwise" scaling dimension was suggested by Farmer et al. (1983) to calculate the D2 for biological data since it does not presume stationarity because nref remains fixed for each D2 estimate. The difference-vectors made with respect to this single nref still span and probe the entire data stream, but they alone are the basis for the log – log plot and the consequent slope and *m* pairs. As nref is chosen sequentially for each digitized point in the time-series, dimension thus is estimated as a function of time.

The „point-D2" (PD2i) estimate of the correlation dimension was developed by Skinner et al. (Skinner et al., 1991; Skinner and Molnár, 1999). The point-D2 does *not* use all possible vector-differences, like the Grassberger and Procaccia algorithm, nor all vector-differences with respect to a fixed nref, like the pointwise algorithm; rather it rejects those nref vector-differences for which linear scaling and smooth convergence cannot be found. Accepting every data-points as an nref means erroneously including those vectors for which the relationship

$$C(r,n)=r^{D2}$$

does not hold. In other words, the dimension cannot be estimated at some nrefs because the data points, being finite, are not distributed on the *m*-dimensional „strange-attactor" in a manner suitable for estimating the correlation dimension starting at that particular nref. The model for the point-D2 is

$$C(r,n,nref^*)= r^{D2}$$

where nref* passes two criteria: (a) linear scaling in the log C(r,n,nref) versus log r plots and (b) convergence of slope versus *m*.

The value of τ is irrelevant only if the number of points in the time-series is infinite, which condition is never approached for biological data. A conventional way of determining the τ to use is to calculate the first zero crossing of the autocorrelation function of the data time-series (i.e., approximately one quarter cycle of the dominant frequency). One should be cautious about new τ requirements when non-stationarities arise in finite data; the autocorrelation function and τ selection should be evaluated for each subepoch.

PD2i parameters

If recordings are made from a sine-wave generator that is suddenly replaced by, for instance, a Lorenz chaotic generator, then nonstationarity will occur in the data stream. Formally, the statistical properties of the data will be different the moment after the replacement. Skinner's laboratory developed the PD2i algorithm to address data nonstationarity, because this problem invariably arises in long epochs of biological data when the system uncontrollably changes state (e.g. in the shifts from sleeping to waking, or from quiescence to alertness). The first insight that led to their algorithm was that, in nonstationary data, the vectors made from 'points' of data that are stationary with respect to the 'point' that the reference vector is in (a 'point' is a small strip of data, $m*\tau$ data points long) will contribute uncontaminated vector-difference lengths only to the small log *r* part of the scaling region.

Skinner et al. (1994) found that this restricted segment could be defined by a linearity criterion (LC) and a plot length (PL) criterion. The LC permits detection of the upper limit of the floppy tail, and the PL sets the upper limit of the restriction (usually 15%, starting from the small log *r* end). To prove that this insight about this restriction was valid, they tested the PD2i algorithm with obviously nonstationary data made from concatenated samples of sine, Lorenz, Henon and random data. It was found that the mean PD2i of each sub-epoch had an error that was < 4% of that made by D2 for the stationary variety of the data (Skinner et al., 1994).

The PD2i program used for nonlinear analysis of the data was provided by courtesy of JE Skinner. First, from the segments of four channels, single channels were isolated because of the requirements of the PD2i calculation program used. At the beginning of the program run, an autocorrelation and power spectral analysis was performed to obtain the τ value for the time delay embedding, which is essential for correct estimation of the attractors. The τ

value at the first zero crossing of the autocorrelation function was selected to acquire statistically independent (i.e. uncorrelated) points for the reliable construction of an attractor in the *m*-dimensional space for the given EEG signal.

After the PD2i calculations for the whole segment of one channel, two diagrams were obtained. One was the compressed original EEG signal under study. The other diagram depicted the 'cloud' of individual values of the point correlation dimension in the same time resolution as the EEG signal above.

The PD2i values were characterized in two different ways. First, a qualitative assessment was made by visual observation of the behavior of the PD2i points. The quantitative analysis was performed by comparison of the histograms derived from the correlation dimension points of the epochs. After selection of an epoch by its starting and end points, the program was able to provide the distribution of the PD2i values within the time window given. The histograms yielded the peak, the average and standard deviation of the point correlation dimension values in the histogram. The percentage of accepted points was also given, which is informative on the stationarity of the analyzed signal.

The parameters used in the current study were PL = 0.15, LC = 0.3, convergence criterion (*m* vs. slope) = 0.4, and $\boldsymbol{\tau}$ was selected at the first zero crossing of the corresponding autocorrelogram (see above). These are the same PD2i settings as used previously in both animal (Skinner et al., 1991; 1994; 1999) and human studies (Skinner et al., 1993; Vybiral and Skinner, 1993).

3.6.3. Synchronization likelihood

Mathematical background of synchronization likelihood (cited from Ponten et al., 2007)

The synchronization likelihood (SL) is a measure of the *generalized synchronization* between two dynamical systems *X* and *Y* (Stam and van Dijk, 2002). Generalized synchronization (Rulkov et al., 1995) exists between *X* and *Y* of the state of the response system is a function of the driver system: $Y = F(X)$. The first step in the computation of the synchronization likelihood is to convert the time series x_i and y_i recorded from *X* and *Y* as a series of state space vectors using the method of time delay embedding (Takens, 1981):

$$X_i = \left(x_i, x_{i+L}, x_{i+2\times L}, x_{i+3\times L} \cdots, x_{i+(m-1)\times L}\right)$$

where L is the time lag, and m is the embedding dimension. From a time series of N samples, $N-(m \times L)$ vectors can be reconstructed. State space vectors Y_i are reconstructed in the same way. Synchronization likelihood is defined as the conditional likelihood that the distance between Y_i and Y_j will be smaller than a cutoff distance r_y, given that the distance between X_i and X_j is smaller than a cutoff distance r_x. In the case of maximal synchronization this likelihood is 1; in the case of independent systems, it is a small, but nonzero, number, namely P_{ref}. This small number is the likelihood that two randomly chosen vectors Y (or X) will be closer than the cut-off distance r. In practice, the cut-off distance is chosen such that the likelihood of random vectors being close is fixed at P_{ref}, which is chosen the same for X and for Y. To understand how P_{ref} is used to fix r_x and r_y we first consider the correlation integral:

$$C_r = \frac{2}{N(N-w)} \sum_{i=1}^{N} \sum_{j=i+w}^{N-w} \theta(r - |X_i - X_j|) \qquad (2)$$

Here the correlation integral Cr is the likelihood that two randomly chosen vectors X will be closer than r. The vertical bars represent the Euclidean distance between the vectors. N is the number of vectors, w is the Theiler correction for autocorrelation (Theiler, 1986) and θ is the Heaviside function: $\theta(X) = 0$ if $X >= 0$ and $\theta(X) = 1$ if $X < 0$. Now, r_x is chosen such that $Cr_x = P_{\text{ref}}$ and r_y is chosen such that $Cr_y = P_{\text{ref}}$. The synchronization likelihood between X and Y can now be formally defined as:

$$SL = \frac{2}{N(N-w)p_{ref}} \sum_{i=1}^{N} \sum_{j=i+w}^{N-w} \theta(r_x - |X_i - X_j|)\theta(r_y - |Y_i - Y_j|) \qquad (3)$$

SL is a symmetric measure of the strength of synchronization between X and Y ($SL_{XY} = SL_{YX}$). In equation (3) the averaging is done over all i and j; by doing the averaging only over j SL can be computed as a function of time i. From (3) it can be seen that in the case of complete synchronization SL = 1; in the case of complete independence $SL = P_{\text{ref}}$. In the case of intermediate levels of synchronization $P_{\text{ref}} < SL < 1$. In the present study the following parameters were used: P_{ref} was set at 0.01, for the state space embedding a time lag of 10 samples, an embedding dimension of 10 and a Theiler correction (W2) of 0.1. When we tried the algorithm proposed by Montez et al. (2006), the results were comparable.

3.7. Statistical analysis

The SL and power spectrum calculation results and the PD2i changes were analyzed by the non-parametric Wilcoxon Signed Rank Test because of its robustness. The distribution of the grand average SL values became normalized by the averaging, therefore we analyzed them by one way ANOVA and subsequent pair wise comparisons of Student t-test where pre- and two post-stimulus values were compared.

Because of the multiple comparisons the row p-values were corrected by false discovery rate (FDR) method. Statistical significance was set at $p<0.05$.

4. Results

4.1. Olfactory and taste stimulation

4.1.1. Subjective report after smell and taste stimulation

After every stimulation record a pleasant-unpleasant scale was given to the patients (the scale was from 1 (bad) to 10 (excellent)). The average of the smell pleasantness was 8 (range 6-10), the taste average was 7.5 (range 5-10).

4.1.2. Analysis of PD2i after smell and taste stimulation

The most important observation of our PD2i study was that after smell stimulation a short lasting, but immediate reaction was found on both sides; in contrast, the effect of taste stimulation was seen later and appeared mainly on the right side *(Fig. 2 (A),(F))*.

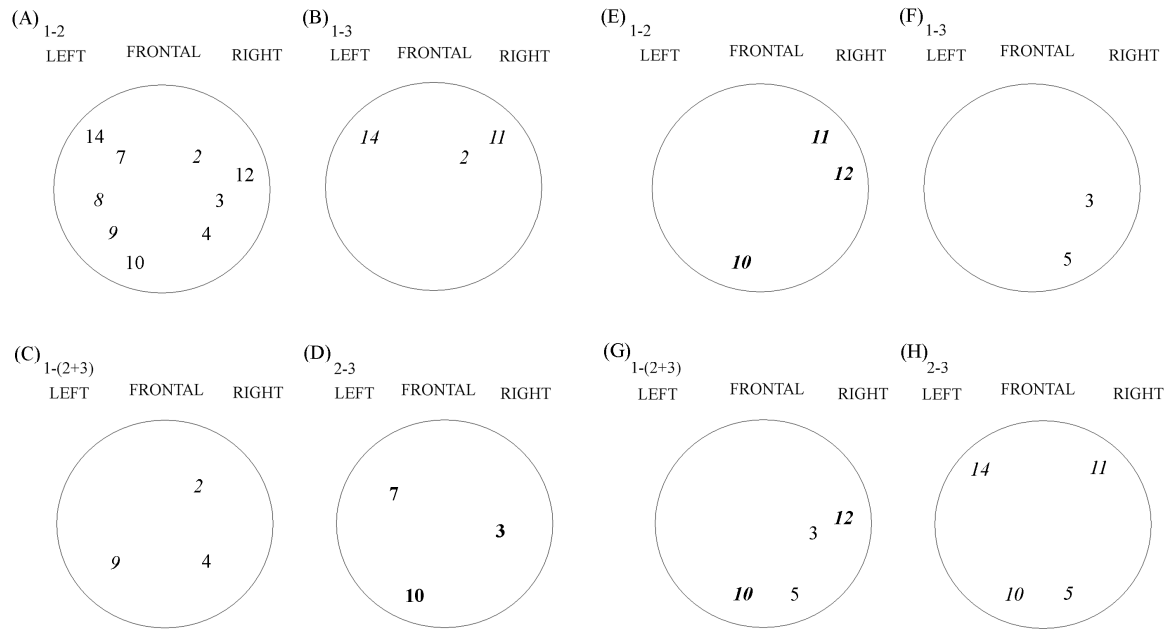

Fig. 2. Significant mean and standard deviation changes of Point Correlation Dimension (PD2i) between control condition and first 15s smell stimulation (A), control condition and second 15s (B), control condition and whole (15+15)=30s activation (C), and between first and second 15s stimulation period (D) as well as between control condition and first 15s taste stimulation (E), control condition and second 15s (F), control condition and whole (15+15)=30s activation (G), and between first and second 15s stimulation (H). Mean decreases are denoted with normal characters; mean increases with **bold**; SD decreases with *italic*; and SD increases with ***bold italic*** letters. Significance set at $p<0.05$.

During the detailed analysis of the smell stimulation, first the mean PD2i decreased from resting state to first 15s, and afterwards, we found an increase between first 15s to second 15s of the activation. There was no significant difference in the mean PD2i between the control condition and the whole 30s after smell stimulation.

The localizational features of PD2i changes after olfactory stimulation are shown in *Fig. 2(A),(B),(C),(D)*: the mean PD2i decreased significantly from pre-smelling baseline to first 15s activation in the left fronto-occipital (7, 14, and 10), and in the right temporo-parieto-central (3, 12, and 4) leads. The standard deviation (SD) of the PD2i histogram also decreased in 2, 3 and 8, 9. Between control condition versus the second 15s activation, only the SD changed significantly on both sides mainly in the anterior parts (2, 11, 14). Between the first and second 15s activation, the mean of the PD2i significantly increased in the fronto-occipital (7, 10) leads on the left, and central leads on the right side (3). Between the control condition and the whole 30s stimulation, the only significant change was a decrease in one lead (4), but the SD decreased in both sides (2, 9).

In contrast, during taste stimulation with a piece of chocolate *(Fig. 2(E),(F),(G),(H))*, significantly lower PD2i mean values were found on the right side between baseline and second 15s epoch alone (3, 5). Comparing the baseline to the first 15s, there was no change in the mean values, but the SD values have increased (11, 12 and 10). The SD was also higher between baseline and the whole 30s stimulation (12, 10), and lower between the first and second 15s (14, 11, 10 and 5).

4.1.3. Synchronization likelihood analysis after smell and taste stimulation

Fig. 3. shows the comparison of the grand average SL values. During the first 15s after both olfactory and gustatory stimulation the SL decreased in the slow alpha band. The decrease of the grand average SL values in the fast alpha was significant only after olfactory stimulation. Later (during the second 15s) a very appreciable SL increase was seen in all of the frequency ranges, especially in beta and gamma bands.

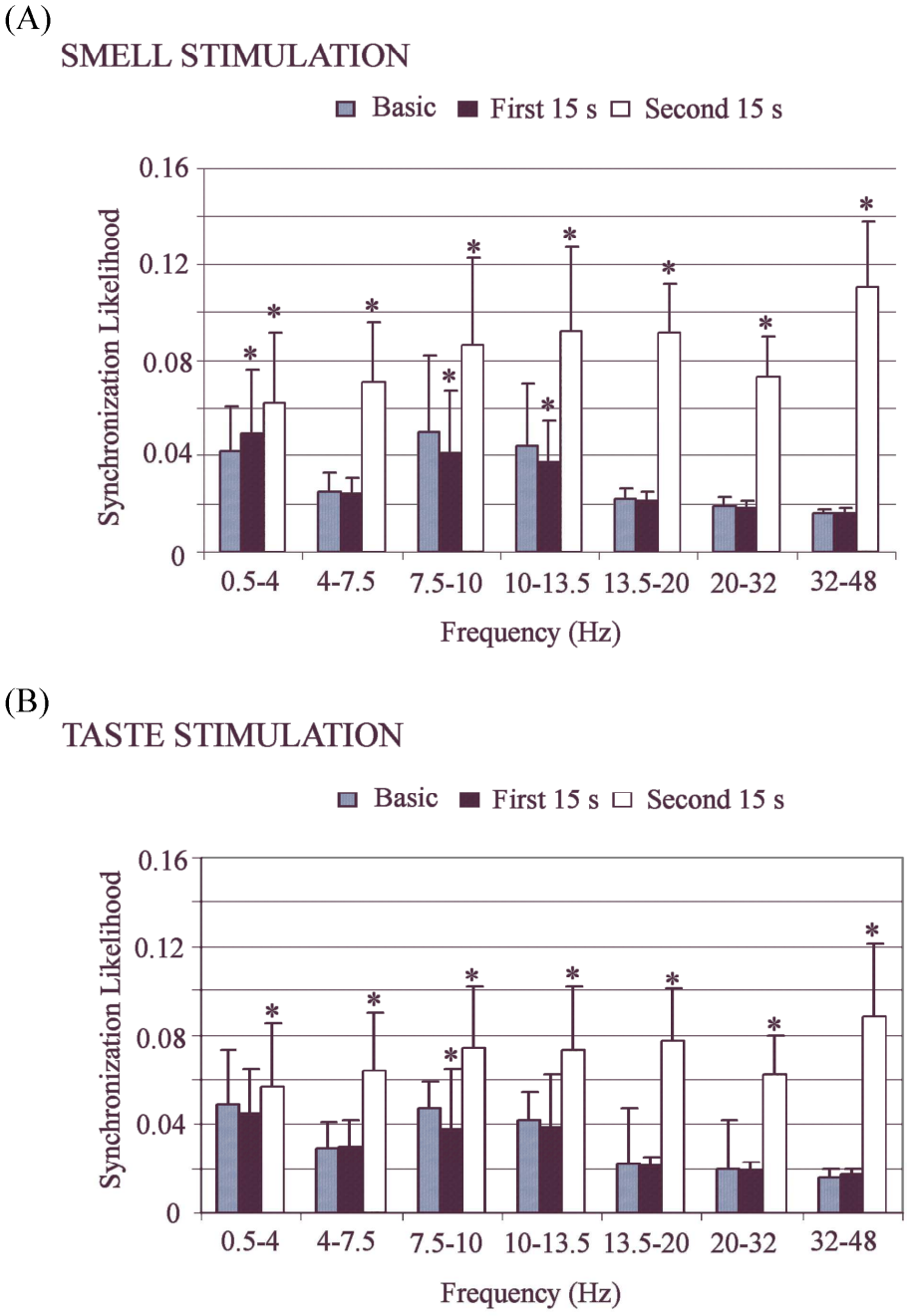

Fig. 3. Grand mean synchronization likelihood (SL) in different frequency bands during basic condition (gray column), after the first 15s (black column) and second 15s (white column) smell (A) or taste (B) stimulations. * highlights significant changes in comparison to the baseline at $p<0.05$

Fig. 4(A) and *(B)* represent the topography of the <u>average SL.</u> It showed some similarities between the two sensory modalities in the 7-14 Hz frequency range as follows: the connections between the different areas disappeared in the first 15s of the stimulation but reappeared on the second 15s. Anterior-temporal to central (14-7 ch) and middle-temporal to occipital connections (15-10 ch) were active during the first 15s. In other bands only small differences were found after stimulations. Both in the 0.5-7 Hz and the 14-30 Hz frequency ranges, the mean SL seemed to have a temporo-occipital dominance. In the left fronto-central area (7-8 ch) the interconnections became stronger in the gamma band, a little earlier after olfactory than in gustatory stimulations.

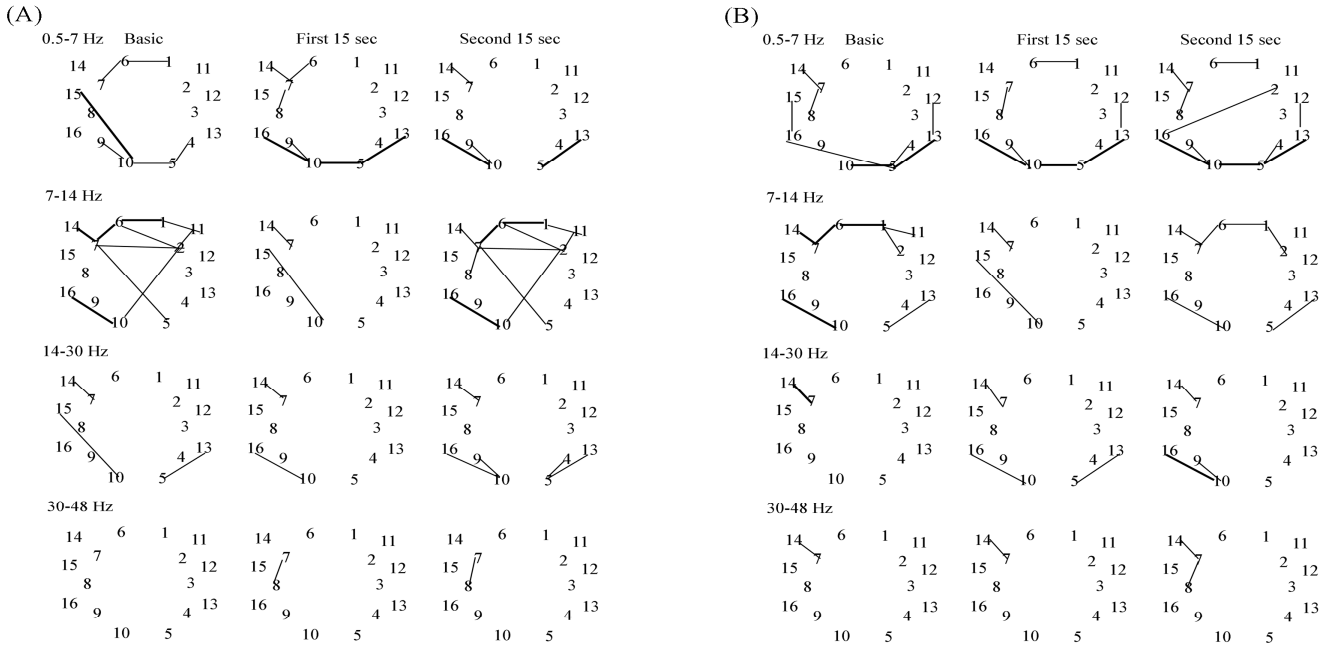

Fig. 4. Average level of synchronization likelihood in different frequency bands before (Basic), in the first and second post-stimulus 15s periods of <u>olfactory (A) and gustatory (B) stimulations</u>. The thick lines (_____) represent SL values > 0.15 , the thin ones (_____) average SL values 0.15> x > 0.08 .

Figs. 5 and *6* demonstrate the topographic results of the statistical analysis in the <u>SL changes</u>. The 7-14 Hz seemed to be the most important frequency range during both smell and taste stimulation, where the strength of the neuronal interconnections reflected in the SL values significantly decreased after 15s stimulation (1-2) in both inter- and intra-

hemispherical localizations. This is one of the main characteristic findings of this SL study. During the second 15s activation, a significant SL increase has appeared in relation to the control condition during smell stimulation *(Fig. 5(A), (B))*; in contrast, during taste stimulation, the SL values significantly decreased. In higher frequencies (14-30 Hz and 30-48 Hz) significant SL increases were observed in the second period after olfactory stimulation (1-3) with inter-hemispherical dominance (*Fig. 6(A), (B))*.

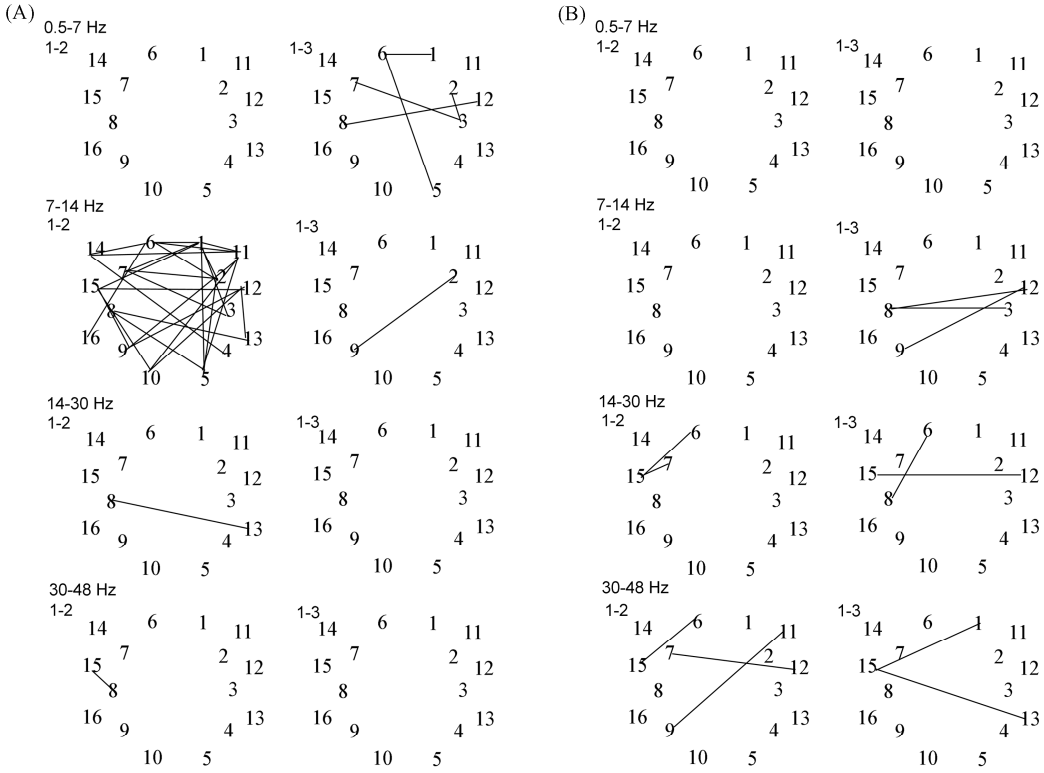

Fig 5. Significant decreases (A) and increases (B) of the interconnections (SL) between different EEG localizations from control condition to first (1-2) and second (1-3) 15s periods of olfactory stimulation. The thick lines (_____) represent connection changes at the level of $p<0.01$, the thin ones (_____) at the level of $p<0.05$.

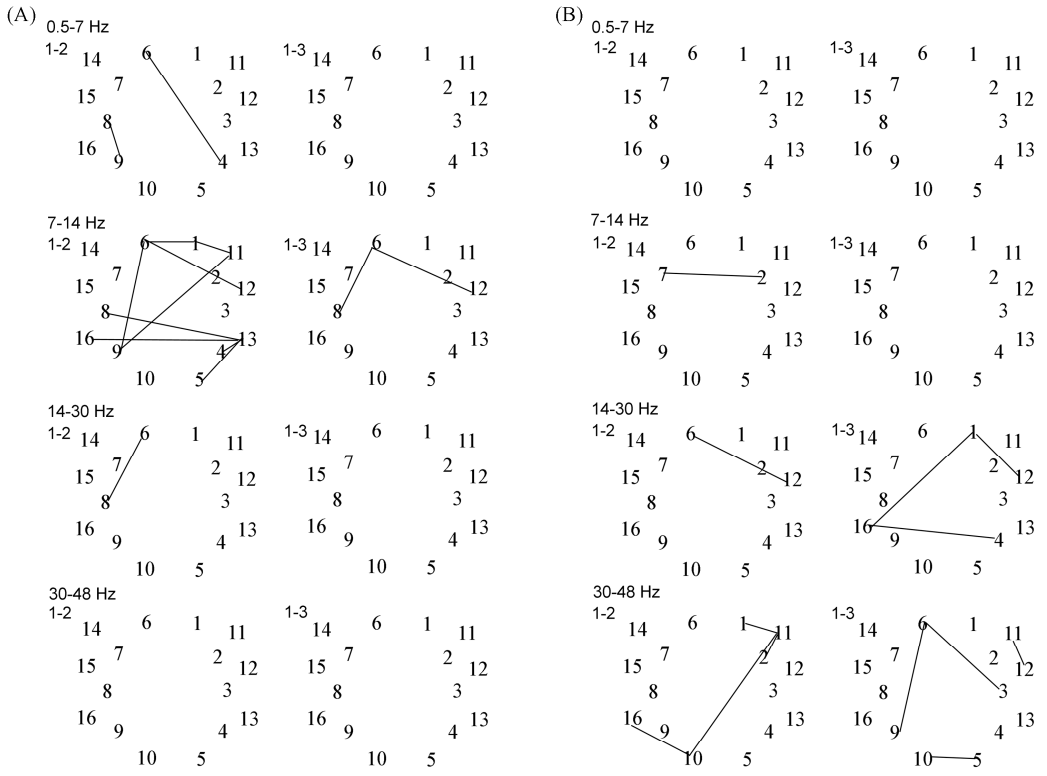

Fig. 6. Significant decreases (A) and increases (B) of the interconnections (SL) between different EEG localizations from control condition to first (1-2) and second (1-3) 15s periods of gustatory stimulation. The thick lines (_____) represent connection changes at the level of $p<0.01$, the thin ones (_____) at the level of $p<0.05$.

After gustatory stimulation there was a frequency shift from lower to higher frequencies compared to the control condition: significant decreases appeared only in the 0.5-7 Hz and the increases in the 30-48 Hz bands. In other ranges and conditions (e.g. olfactory stimulation: 0.5-7 Hz: 1-2, 1-3 (characteristic decrease); 14-30 Hz and 30-48 Hz: 1-2; gustatory stimulation: 14-30 Hz: 1-2) the changes were not so representative. Both SL increases and decreases appeared between different inter- and intra-hemispherical localizations.

4.2. Quantitative EEG changes in Alzheimer's patients after lactate infusion

4.2.1. Spectral analysis in AD patients before and after lactate infusion

Fig. 7. summarizes our major findings on the relative band power values.

(a)

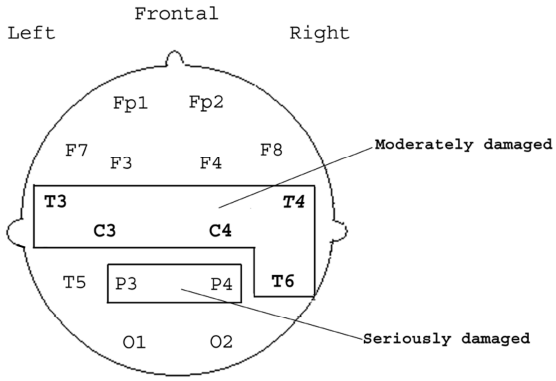

(b)

	0.5-4 Hz	4-8 Hz	8-12 Hz	12-20 Hz	20-30 Hz	30-48 Hz
Fp1	**0.0930**	0.1479	0.0645	0.0614	0.1479	0.1380
Fp2	**0.1256**	0.1462	0.1342	0.0614	0.1479	0.1380
F3	**0.0850**	0.1479	0.1342	0.0684	0.1479	0.1380
F4	**0.0930**	0.1476	0.0860	0.1479	0.1479	0.1380
F7	**0.1514**	0.1479	0.1763	0.1465	0.1479	0.1380
F8	**0.1380**	0.1476	0.1763	0.1763	0.1479	0.1380
T3	**0.0109***	0.1479	0.1342	0.0130*	0.1479	0.1380
T4	**0.0109***	0.1462	0.1342	0.0614	0.1479	0.1380
C3	**0.0109***	0.1462	0.1465	0.0137*	0.1479	0.1380
C4	**0.0109***	0.0547	0.0234*	0.0130*	0.0391*	0.1380
T5	**0.0929**	0.1462	0.1342	0.1615	0.1479	0.1380
T6	**0.0109***	0.1462	0.0645	0.0130*	0.1479	0.1514
P3	**0.1136**	0.1514	0.1763	0.1479	0.1514	0.1380
P4	**0.0850**	0.1514	0.1763	0.1465	0.1514	0.1380
O1	**0.1136**	0.1462	0.0645	0.1234	0.1479	0.1380
O2	**0.0850**	0.1476	0.1342	0.1234	0.1479	0.1380

Fig. 7. **(a)** Topographic view of scalp electrode positions used in this study. The **bold** letters here represent the channels where the relative power increase in the delta band after sodium lactate infusion was accompanied by power decrease in the higher frequency range**.** The *T4* shows a localization where only significant relative delta power decrease was found.

(b) p-values of the relative power changes corrected by false discovery rate (FDR) method after lactate infusion in six frequency bands and sixteen channels found by non-parametric Wilcoxon signed rank test. **Bold** letters in the delta band represent increases, all others show decreases. The * denotes localizations where the changes were significant at the level of $p<0.05$.

The main relevant observation was seen on certain scalp localizations (C3, C4, T3, T6) where the delta increase was combined with decrease in the theta, alpha, beta1 or beta2 bands, which were highlighted on *Fig. 7.* by bold letters as well. The most characteristic changes were at C4 where the concomitant significant decreases were seen in three (alpha, beta1 and beta 2) bands. At the C3, T3 and T5 the decreases were only in the beta1 band. In the T4 localization only a significant delta increase has appeared.

At frontal (Fp1, F3) as well as in occipital (O1) localizations non-significant decreases were found in the left side at. Similarly, on the right side the frontal (Fp2, F4) and T4 leads showed tendency of decrease in alpha and/or beta1 band power values. The very fast components (beta2 and gamma) of the EEG activity had some non-significant decreases mainly in the right central (C4) and frontal (Fp2) leads.

4.2.2. Synchronization likelihood analysis in AD patients before and after lactate infusion

In AD patients the grand average of the SL was at about ten times higher in the 0.5-4 Hz frequency band than in all other bands either before or after lactate infusion. Theta (4-7 Hz) and alpha 1-2 (7-10 Hz, 10-13 Hz) frequency bands *(Fig. 8.)* had slightly higher grand mean values than in the higher frequency bands (13-20 Hz, 20-30 Hz, 30-48 Hz). No significant changes were found between the grand average values before and after lactate in any frequency band.

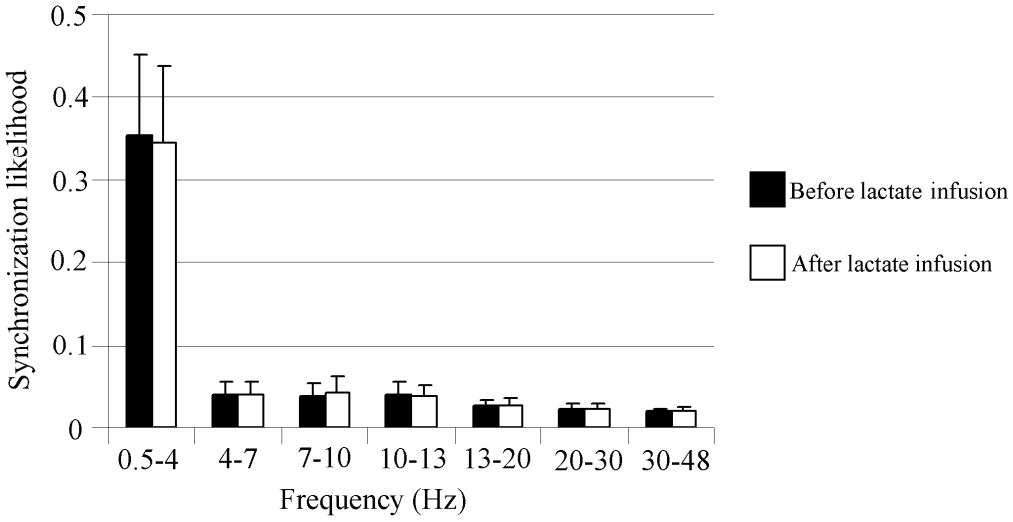

Fig. 8. Grand average and SD values of the synchronization likelihood before and after sodium lactate infusion. Please note that the mean SL in the delta band (with its 0.35 value) is many times higher than in all other frequency bands which show a little higher values in the 4-13Hz than in the 13-48 Hz range. There are no significant changes in the grand mean at any frequency band before and after lactate infusion.

We did not expect systematic reactions after lactate in our patients because of the observed variability of the SL values. However, we were interested in the SL changes at the right fronto-polar (Fp2) region, which was found to be spectrally non-reactive similarly to the seriously damaged P3-P4 area. Our SL analysis revealed a visible frequency shift from lower to higher frequency bands on the right side in Fp2 *(Fig. 9)*, the interconnections of the slow generators in the 4-7 Hz band decreased (a) and the fast connections in the 13-20 Hz range increased (b). It is important to highlight, that there were no changes in the seriously affected parietal leads (P3 and P4) as well.

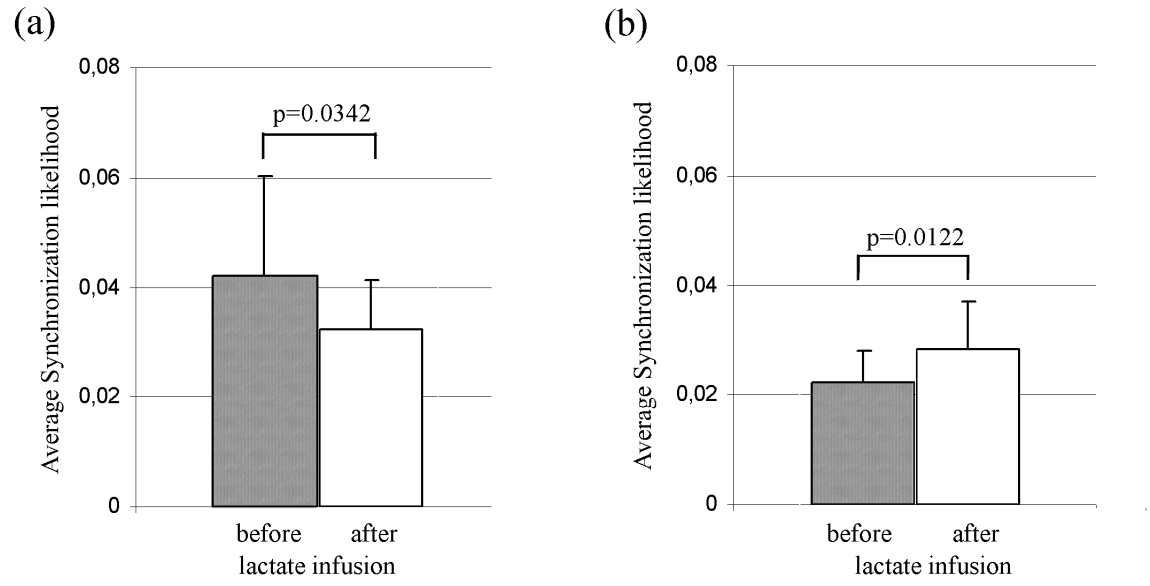

Fig. 9. The average and SD synchronization likelihood values in the right fronto-polar (Fp2) leads before and after sodium lactate infusion in the (a) theta (4-7 Hz) and (b) beta1 (13-20 Hz) frequency bands. The changes were significant by Wilcoxon signed rank test at the false discovery rate (FDR) corrected probability level set at $p<0.0375$.

5. Discussion

5.1. Olfactory and taste stimulation

5.1.1. Point correlation dimensional changes after smell and taste stimulation

During our PD2i analysis we found significantly lower mean values after the appearance of both chemical sensations compared to the control condition. The less complex brain activity denoted in the decreased mean PD2i activity is probably the sign of pre-stimulation processing. This may be related to the changes in ’cooperation’ among the underlying cortical neurons that assist in the electrical reaction after conditioned stimuli (Skinner and Molnár, 1999). The lower correlation dimension could also be the consequence of the relaxed state of the brain after sound or reflexologic stimulation (Kannathal et al., 2004b). These changes appeared earlier (first 15s) after smell and later (30s) after taste stimulation. The difference between the time courses of the two different sensations might be interpreted either by the different chemical pathways or by our experimental protocol. The smell was felt immediately after the presentation; taste, however, only after the chocolate dissolved. Smell sensation and perception caused significantly higher mean PD2i values in the second 15s activation compared to the first 15s, which seemed to be the real effect of the stimulation. This is in concordance with the enhanced cognitive activity and consequently it might be a sign of data processing. No significant increases were found after taste stimulation, possibly because of the above mentioned reasons. Smell stimulation resulted in changes of the correlation dimension at the left fronto-occipital, and right centro-temporo-parietal areas. Kline et al. (2000) found that the activation in the frontal areas is in connection with pleasant smell sensations. The occipital changes could possibly be the projections of the cerebellar activation as well, which would be in turn the consequence of the frontal activation (Smejkal et al., 2003). The right sided activation after taste stimulation is possibly in correlation with memory processes (Royet and Plailly, 2004).

5.1.2. Synchronization likelihood changes after smell and taste stimulation

The dominant rhythm of these healthy subjects was in the alpha and delta bands and was reflected in the highest mean SL values in the control condition. The SL values were significantly lower in the alpha band during the first 15s activation. This is possibly the consequence of a pleasant stimulus (Masago et al., 2000) or could be explained by the use of the working memory (Stam et al., 2002). These processes could be defined with less complex neuronal interconnections, during this period the brain is preparing for data processing. In our

concept the lower SL would mean less coupling or more independent brain networks. This could be confirmed by the localizational features of the mean SL. Many connections disappeared in the first 15s activation, but reappeared in the second 15s in the 7-14 Hz frequency range. The most intense connections in the alpha band were on the left side in the antero-temporal and central (14-7 ch), middle-temporal and occipital (15-10 ch) connections. These are perhaps responsible for the detection of the early stimulations. Our opinion is that the real data processing of the chemical sensations could be detected with SL method during the second 15s when appreciable elevations of the SL turned up in all bands, especially in the faster frequency (beta and gamma) bands.

The higher gamma synchronization is mainly important in cognitive processes and higher mental functions (Beshel et al., 2007), but it could be associated with the higher activity of the olfactory bulb and/or face muscles represented in the gamma frequency band as well. After gustatory stimulation, lower alpha band synchronization was found only, which is possibly the sign of an incomplete preparation for data processing.

5.2. Quantitative EEG effects in AD patients after lactate infusion

5.2.1. Relative power changes after lactate infusion

The major finding of our present study was that AD patients' brain can be divided into three parts based on the neurophysiological reactivity to sodium lactate: seriously, moderately affected and nearly normal areas. In the most seriously affected areas (P3, P4) no significant changes were found after lactate infusion either in relative power or in SL. The relative non-reactivity to sodium lactate infusion of the seriously damaged parietal areas of the AD patients (P3 and P4) could be interpreted by the disturbed altered synaptic function, which is a characteristic sign of this neurodegenerative disorder (Francis, 2005; Bell et al., 2006) in two different ways: First, the decreased mainly acetylcholinergic innervations of the bilateral parieto-temporal cortex (Schliebs and Arendt, 2006) and the consequent hypometabolism of the same areas have been described by Positron Emission Tomography studies (de Leon et al., 2007). Second, the local hypoperfusion, which is the succeeding of the decreased direct cholinergic vasoreaction (Barbelivien et al., 1999; Sato et al., 2004). This is in possible correlation with the decreased number of projections from the nucleus basalis Meynert (Mattia et al., 2003; Adler, 2000). Abásolo et al. (2005) published that with Aproximate Entropy, significantly lower 'normal' irregularity in P3 and P4 localizations was found with concomitant relative power increase in the delta (T4, P4) and decrease in the alpha (T3, T4) bands in AD patients in comparison with age-matched elderly controls. It is pertinent to

mention here that the decreased ACh-ergic activation could be reflected by the dominance of slow rhythms in the background EEG at and around both parieto-temporal regions (Elmstahl and Rosén, 1997). The insufficient acetylcholinergic innervation (Schliebs and Arendt, 2006) of the parietal (P3, P4) regions in advanced AD might be responsible for the reduced vascular reactivity of the examined brain areas after sodium lactate and might have further influence on the brain circulation and metabolism as it was published in our former SPECT brain imaging study on similar AD population (Kálmán et al., 2005a). This could be a possible explanation why we did not find any significant EEG power and SL changes after the sodium lactate infusion mainly over these brain territories. As a result, no beneficial effect of sodium lactate infusion on semantic categorization was observed in ERP studies by the same group as well (Kálmán et al., 2005b).

In the moderately involved areas, the relative power of the slow generators increased, which is in agreement with the well characterized, but not specific features of the EEG in AD (Elmstahl and Rosén, 1997; Prichep, 2007). The main theta and delta frequency dominance was shifted to delta after the sodium lactate infusion together with an increase in the relative delta band power and a joint decrease in the alpha, beta1, and beta2 bands (*Fig. 7(a)* bold letters, *Fig. 7(b)* stars). This could be interpreted by a partial metabolic and possibly non vascular (Pávics et al., 1999) 'steal' effect of the intact brain areas, presuming that these preserved brain regions has a better response to the supposedly vaso- and metabolic-active sodium lactate infusion than the moderately affected areas.

5.2.2. Synchronization likelihood changes after lactate infusion

The slower dominant frequency of the Alzheimer's patients is one of the characteristic features of their EEGs (Elmstahl and Rosén, 1997). This could be explained by the decrease of the number and activity of the EEG generating elements i.e. neurons and glial cells. Based on this feature it is expected that the majority of the communication between all of these generators is made in this frequency band. This could be one possible cause of the dominance of the grand average SL in the delta (0.5-4.0 Hz) frequency band. The lactate infusion in the dose applied did not change the sum of the communications (grand average SL) either in the delta or faster EEG bands significantly. We think that this finding could be explained by the decreased reactivity of the Alzheimer's brain to metabolic stimulation.

However, the detailed study of the localized and not global SL changes could reveal some differences between regions which showed same i.e. non-detectable spectral reactivity to lactate. The seriously damaged P3, P4 and normal Fp2 activities did not show significant

relative power changes but only this later could present tiny signs of the subtle activation. Our opinion is that the significant decrease of the SL in the lower (theta) and increase in the faster (beta) bands could represent a shift to a stimulated enhanced activity of the Fp2 region.

5.2.3. Methodological problems

One of the major limitations of our second study is that due to ethical considerations we were not able to perform similar experiments on healthy elderly. We can not exclude therefore the possibility that our major findings are not specific to AD and the same steal phenomenon could be observed in healthy aged population after sodium lactate infusion.

6. Conclusions

1. The main important observation of our PD2i study was that the mean values became significantly lower after the appearance of both chemical sensations compared to the control condition, which is probably the sign of the prestimulus processing. The consequences of smell stimulation seemed to be short lasting but immediate, and they appeared on both sides. In contrast, the effect of taste stimulation was a later reaction and it was found mainly on the right i.e. subdominant side.

2. Our SL study presented significantly lower mean values during the first 15s of both chemical activations. The less complex neuronal interconnections could mean that the brain was preparing for the detailed data processing. The localisational features of mean SL could confirm this statement, as some connections disappeared in the first 15s activation, but reappeared in the second 15s in the 7-14 Hz frequency range. The real data processing was in connection with an appreciable mean SL increase during the second 15s in all bands, especially in the faster ones.

3. Based on the spectral reactivity to sodium lactate the AD patients' brain could be divided into three parts: seriously, moderately damaged and nearly normal areas. In the seriously affected areas (P3 and P4) no significant changes were found after lactate infusion either in relative power or in SL, which could be interpreted by the altered synaptic function. In the moderately involved areas, the relative power of the slow generators increased, and the previous theta and delta frequency dominance was shifted to delta, and there was a joint decrease in the alpha, beta1 and beta2 bands. This is possibly the sign of a partial metabolic and possibly non vascular 'steal' effect of the activated intact brain areas where this activation is signed by the significant theta decrease and beta increase of the localized SL values e.g. in the Fp2 region.

4. The above findings give the answers to the questions taken in the Aims chapter are as follows:

A) The local organization measured by mean PD2i changes can reflect the periods of preprocessing and real data processing after olfactory and smell stimulation. These periods

appeared in the global (inter-local) organization as well investigated by individual SL values but they provided additional information on the uni- or bi-lateral nature of the data processing.

B) So we suggest to apply both or at least the SL analysis for the proper collection of a normative database for a later comparison with some neurodegenerative diseases.

C) The spectral analysis of the EEG has proven appropriate in the low metabolic level detection of the differently altered Alzheimer's brains' regions.

D) The combined inter-connectional SL analysis was able to give important information on the higher level activation of the different regions which showed otherwise similar spectral reactions.

5. The main observation of my thesis is that linear 'power spectrum' analysis is the most suitable for the analysis of the metabolic and hemodynamic changes. SL and nonlinear PD2i is more preferable during the analysis of the cognitive functions.

7. Acknowledgements

I would like to express my gratitude to *Professor Dr. László Vécsei*, Chairman of the Department of Neurology, University of Szeged, for his scientific guidance and continuous support, as well as for the opportunity to prepare my Ph.D. thesis in the Department of Neurology.

I am grateful to my supervisor, *Dr. János Tajti*, for organizing my work, and for his scientific guidance.

I wish to thank to *Professor James E Skinner* and *Professor Mark Molnar* for providing the PD2i program for data-processing. I am also especially grateful to *Professor Cornelis J Stam* for his valuable advices in the use of his DigEEGXP program, critical reading of the versions of our manuscripts as well as useful help in the interpretation of synchronization likelihood results.

I wish to thank all my co-workers, especially to *Dr. János Kálmán*, who participated in the sodium lactate experiments; to *Krisztina Boda* PhD for her valuable statistical advices; and all the probands for their participation in our studies.

8. References

Abásolo, D., Hornero, R., Espino, P., Poza, J., Sánchez, C.I. and de la Rosa, R. (2005). Analysis of regularity in the background activity of Alzheimer's disease patients with Approximate Entropy. Clin. Neurophys. 116, 1826-1834.

Adeli, H., Ghosh-Dastidar, S. and Dadmehr, N. (2007). A wavelet-chaos methodology for analysis of EEGs and EEG subbands to detect seizure and epilepsy. IEEE Trans. Biomed. Eng. 54, 205-211.

Adler, G. (2000). The EEG as an indicator of cholinergic deficit in Alzheimer's disease. Fortschr. Neurol. Psychiatrie 68, 352-356.

Aftanas, L.I., Lotova, N.V., Koshkarov, V.I. and Popov, S.A. (1998). Non-linear dynamical coupling between different brain areas during evoked emotions: an EEG investigation. Biol. Psychol. 48, 121-138.

Aihua, Z. and Yuhan, Z. (2005). Phase synchronization analysis and support vector machine for recognition of mental tasks. Conf. Proc. IEEE Eng. Med. Biol. Soc. 5, 5373-5376.

Altenburg, J., Vermeulen, R.J., Strijers, R.L., Fetter, W.P. and Stam, C.J. (2003). Seizure detection in the neonatal EEG with synchronization likelihood. Clin. Neurophysiol. 114, 50-55.

Babiloni, C., Ferri, R., Moretti, D.V., Strambi, A., Binetti, G., Dal Forno, G., Ferreri, F., Lanuzza, B., Bonato, C., Nobili, F., Rodriguez, G., Salinari, S., Passero, S., Rocchi, R., Stam, C.J. and Rossini, P.M. (2004). Abnormal fronto-parietal coupling of brain rhythms in mild Alzheimer's disease: a multicentric EEG study. Eur. J. Neurosci. 19, 2583-2590.

Babloyantz, A., Salazar, J.M. and Nicolis, C. (1985). Evidence of chaotic dynamics of brain activity during the sleep cycle. Phys. Lett. A 111, 152-156.

Barbelivien, A., Bertrand, N., Besret, L., Beley, A., MacKenzie, E.T. and Dauphin, F. (1999). Neurochemical stimulation of the rat substantia innominata increases cerebral blood flow (but not glucose use) through the parallel activation of cholinergic and non-cholinergic pathways. Brain Res. 840, 115-124.

Bartolomei, F., Bosma, I., Klein, M., Baayen, J.C., Reijneveld, J.C., Postma, T.J., Heimans, J.J., van Dijk, B.W., de Munck, J.C., de Jongh, A., Cover, K.S. and Stam, C.J. (2006). Disturbed functional connectivity in brain tumour patients: evaluation by graph analysis of synchronization matrices. Clin. Neurophysiol. 117, 2039-2049.

Bell, K.F. and Claudio Cuello, A. (2006). Altered synaptic function in Alzheimer's disease. Eur. J. Pharm. 545, 11-21.

Beshel, J., Kopell, N. and Kay, L.M. (2007). Olfactory bulb gamma oscillations are enhanced with task demands. J. Neurosci. 27, 8358-65.

Boccaletti, S., Kurths, J., Osipov, G., Valladares, D.L. and Zhou, C.S. (2002). The synchronization of chaotic systems. Phys. Rep. 366, 1-101.

Breakspear, M., Williams, L.M. and Stam, C.J. (2004). A novel method for the topographic analysis of neural activity reveals formation and dissolution of 'dynamic cell assemblies'. J. Comput. Neurosci. 16, 49-68.

Buzug, Th., Pawelzik, K., Stamm, J. and Pfister, G. (1994). Mutual information and global strange attractors in Taylor-Couette flow. Physica D 72, 343-350.

Ciponeriu, L., Rosenblum, M., Fieseler, T., Dammers, J., Schiek, M., Majtanik, M., Morosan, P., Beserianos, A. and Tass, P.A. (2003). Inferring asymmetric relations between interacting neuronal oscillators. Prog. Theor. Phys. Suppl. 22-36.

Czigler, B., Csikós, D., Hidasi, Z., Gaál, A.Z., Csibri, E., Kiss, E., Salacz, P. and Molnár, M. (2008). Quantitative EEG in early Alzheimer's disease patients - power spectrum and complexity features. Int. J. Psychophysiol. 68, 75-80.

Daw, C.S., Finney, C.E. and Kennel, M.B. (2000). Symbolic approach for measuring temporal "irreversibility". Phys. Rev. E Stat. Phys. Plasmas Fluids Relat. Interdiscip. Topics. 62, 1912-1921.

de Leon, M.J., Mosconi, L., Blennow, K., DeSanti, S., Zinkowski, R., Mehta, P.D., Pratico, D., Tsui, W., Saint Louis, L.A., Sobanska, L., Brys, M., Li, Y., Rich, K., Rinne, J. and Rusinek, H. (2007). Imaging and CSF studies in the preclinical diagnosis of Alzheimer's disease. Ann. N.Y. Acad. Sci. 1097, 114-145.

Duhamel, P. and Vetterli, M. (1990). Fast Fourier transforms: a tutorial review and state of the art. Signal Process. 19, 259-299.

Elmstahl, S. and Rosén, I. (1997). Postural hypotension and EEG variables predict cognitive decline: results from a 5-year follow-up of healthy elderly women. Dement. Geriatr. Cogn. Dis. 8, 180-187.

Farmer, J.D., Ott, E. and Yorke, J.A. (1983). The dimension of chaotic attractors. Physica 7D 153-180.

Ferri, R., Chiaramonti, R., Elia, M., Musumeci, S.A., Ragazzoni, A. and Stam, C.J. (2003). Nonlinear EEG analysis during sleep in premature and full-term newborns. Clin. Neurophysiol. 114, 1176-80.

Ferri, R., Elia, M., Musumeci, S.A. and Stam, C.J. (2001). Non-linear EEG analysis in children with epilepsy and electrical status epilepticus during slow-wave sleep (ESES). Clin. Neurophysiol. 112, 2274-2280.

Ferri, R., Parrino, L., Smerieri, A., Terzano, M.G., Elia, M., Musumeci, S.A., Pettinato, S. and Stam, C.J. (2002). Non-linear EEG measures during sleep: effects of the different sleep stages and cyclic alternating pattern. Int. J. Psychophysiol. 43, 273-286.

Ferri, R., Stam, C.J., Lanuzza, B., Cosentino, F.I., Elia, M., Musumeci, S.A. and Pennisi, G. (2004). Different EEG frequency band synchronization during nocturnal frontal lobe seizures. Clin. Neurophysiol. 115, 1202-1211.

Francis, P.T. (2005). The interplay of neurotransmitters in Alzheimer's disease. CNS Spectrums 10, 6-9.

Gifani, P., Rabiee, H.R., Hashemi, M. and Ghanbari, M. (2007). Dimensional characterization of anesthesia dynamic in reconstructed embedding space. Conf. Proc. IEEE Eng. Med. Biol. Soc. 2007, 6484-6487.

Grassberger, P. and Procaccia, I. (1983a). Measuring the strangeness of the strange attractors. Physica D 9, 189-208.

Grassberger, P. and Procaccia, I. (1983b). Characterization of strange attractors. Phys. Rev. Lett. 50, 448-451.

Hidasi, Z., Czigler, B., Salacz, P., Csibri, E. and Molnár, M. (2007). Changes of EEG spectra and coherence following performance in a cognitive task in Alzheimer's disease. Int. J. Psychophysiol. 65, 252-260.

Janjarasjitt, S., Scher, M.S. and Loparo, K.A. (2008a). Nonlinear dynamical analysis of the neonatal EEG time series: the relationship between neurodevelopment and complexity. Clin. Neurophysiol. 119, 822-836.

Janjarasjitt, S., Scher, M.S. and Loparo, K.A. (2008b). Nonlinear dynamical analysis of the neonatal EEG time series: the relationship between sleep state and complexity. Clin. Neurophysiol. 119, 1812-1823.

Járdánházy, A., Molnár, M. and Járdánházy, T. (2007). Point correlation dimension can reveal functional changes caused by gap junction blockers in the 4-aminopyridine in vivo rat epilepsy model. Chaos Soliton. Fract. In Press.

Járdánházy, A., Járdánházy, T. and Kálmán, J. (2008). Sodium lactate differently alters relative EEG power and functional connectivity in Alzheimer's disease patients' brain regions. Eur. J. Neurol. 15, 150-155.

Jelles, B., Scheltens, P., van der Flier, W.M., Jonkman, E.J., da Silva, F.H. and Stam, C.J. (2008). Global dynamical analysis of the EEG in Alzheimer's disease: frequency-specific changes of functional interactions. Clin. Neurophysiol. 119, 837-841.

Kálmán, J., Palotás, A., Bódi, N., Kincses, T.Z., Benedek, G., Janka, Z. and Antal, A. (2005a). Lactate infusion fails to improve semantic categorization in Alzheimer's disease. Brain Res. Bull. 65, 533-539.

Kálmán, J., Palotás, A., Kis, G., Boda, K., Túri, P., Bari, F., Domoki, F., Dóda, I., Árgyelán, M., Vincze, G., Séra, T., Csernay, L., Janka, Z. and Pávics, L. (2005b). Regional cortical blood flow changes following sodium lactate infusion in Alzheimer's disease. Eur. J. Neurosci. 21, 1671-1678.

Kannathal, N., Paul, J.K., Lim, C.M. and Chua, K.P. (2004b). Effect of reflexology on EEG--a nonlinear approach. Am. J. Chin. Med. 32, 641-650.

Kannathal, N., Puthusserypady, S.K. and Choo Min, L. (2004a). Complex dynamics of epileptic EEG. Conf. Proc. IEEE Eng. Med. Biol. Soc. 1, 604-607.

Kline, J.P., Blackhart, G.C., Woodward, K.M., Williams, S.R. and Schwartz, G.E. (2000). Anterior electroencephalographic asymmetry changes in elderly women in response to a pleasant and an unpleasant odor. Biol. Psychol. 52, 241-250.

Kozma, R. and Freeman, W.J. (2002). Classification of EEG patterns using nonlinear dynamics and identifying chaotic phase transitions. Neurocomputing 1107-1112.

Kurova, N.S. and Cheremushkin, E.A. (2007). Spectral EEG characteristics during increases in the complexity of the context of cognitive activity. Neurosci. Behav. Physiol. 37, 379-385.

Lachaux, J.P., Rodriguez, E., Martinerie, J. and Varela, F.J. (1999). Measuring phase synchrony in brain signals. Hum. Brain Mapp. 8, 194-208.

Lalitha, V. and Eswaran, C. (2007). Automated detection of anesthetic depth levels using chaotic features with artificial neural networks. J. Med. Syst. 31, 445-452.

Lee, H.C., van Drongelen, W., McGee, A.B., Frim, D.M. and Kohrman, M.H. (2007). Comparison of seizure detection algorithms in continuously monitored pediatric patients. J. Clin. Neurophysiol. 24, 137-146.

Li, T.Y. and Yorke, J.A. (1975). Period three implies chaos. Am. Math. Monthly 82, 985-992.

Lorenz, E.N. (1963). Deterministic nonperiodic flow. J. Atmos. Sci. 20, 130-141.

Masago, R., Matsuda, T., Kikuchi, Y., Miyazaki, Y., Iwanaga, K., Harada, H. and Katsuura, T. (2000). Effects of inhalation of essential oils on EEG activity and sensory evaluation. J. Physiol. Anthropol. Appl. Human Sci. 19, 35-42.

Mattia, D., Babiloni, F., Romigi, A., Cincotti, F., Bianchi, L., Sperli, F., Placidi, F., Bozzao, A., Giacomini, P., Floris, R. and Grazia Marciani, M. (2003). Quantitative EEG and dynamic susceptibility contrast MRI in Alzheimer's disease: a correlative study. Clin. Neurophys. 114, 1210-1216.

Meng, X., Xu, J. and Gu, F. (2001). Generalized dimension of the intersection between EEGs. Biol. Cybern 85, 313-318.

Meyer-Lindenberg, A., Bauer, U., Krieger, S., Lis, S., Vehmeyer, K., Schüler, G. and Gallhofer, B. (1998). The topography of non-linear cortical dynamics at rest, in mental calculation and moving shape perception. Brain Topogr. 10, 291-299.

Micheloyannis, S., Pachou, E., Stam, C.J., Breakspear, M., Bitsios, P., Vourkas, M., Erimaki, S. and Zervakis, M. (2006). Small-world networks and disturbed functional connectivity in schizophrenia. Schizophr. Res. 87, 60-66.

Molnár, M., Csuhaj, R., Horváth, S., Vastagh, I., Gaál, Z.A., Czigler, B., Bálint, A. and Nagy, Z. (2006a). Changes in EEG-complexity after subcortical ischemic brain damage. Ideggyogy. Sz. 59, 185-192.

Molnár, M., Csuhaj, R., Horváth, S., Vastagh, I., Gaál, Z.A., Czigler, B., Bálint, A., Csikós, D. and Nagy, Z. (2006b). Spectral and complexity features of the EEG changed by visual input in a case of subcortical stroke compared to healthy controls. Clin. Neurophysiol. 117, 771-780.

Montez, T., Linkenkaer-Hansen, K., van Dijk, B.W. and Stam, C.J. (2006). Synchronization likelihood with explicit time-frequency priors. Neuroimage 33, 1117-1125.

Mormann, F., Lehnertz, K., David, P. and Elger, C.E. (2000). Mean phase coherence as a measure for phase synchronization and its application to the EEG of epilepsy patients. Physica D 144, 358-369.

Nuwer, M.R. (1988). Quantitative EEG: I. Techniques and problems of frequency analysis and topographic mapping. J. Clin. Neurophys. 5, 1-43.

Otto, K.A. (2008). EEG power spectrum analysis for monitoring depth of anaesthesia during experimental surgery. Lab. Anim. 42, 45-61.

Packard, N., Crutchfield, J., Farmer, D. and Shaw, R. (1980). Geometry from a time series. Phys. Rev. Lett. 45, 712-715.

Pávics, L., Grünwald, F., Reichmann, K., Horn, R., Kitschenberg, A., Hartmann, A., Menzel, C., Schomburg, A.G., Overbeck, B., Csernay, L. and Biersack, H.J. (1999). Regional cerebral blood flow single-photon emission tomography with 99mTc-HMPAO and the

acetazolamide test in the evaluation of vascular and Alzheimer's dementia. Eur. J. Nucl. Med. 26, 239-245.

Pijnenburg, Y.A., van der Made, Y., van Cappellen van Walsum, A.M., Knol, D.L., Scheltens, P. and Stam, C.J. (2004). EEG synchronization likelihood in mild cognitive impairment and Alzheimer's disease during a working memory task. Clin. Neurophysiol. 115, 1332-1339.

Ponten, S.C., Bartolomei, F. and Stam, C.J. (2007). Small-world networks and epilepsy: graph theoretical analysis of intracerebrally recorded mesial temporal lobe seizures. Clin. Neurophysiol. 118, 918-927.

Prichep, L.S. (2007). Quantitative EEG and electromagnetic brain imaging in aging and in the evolution of dementia. Ann. N.Y. Acad. Sci. 1097, 156-167.

Rajna, P. (2006). Mégis Hans Bergernek lesz igaza? Adatok a korszerű klinikai electroencephalographia pszichiátriai jelentőségéhez. Orvosképzés 1, 1-68.

Rapp, P.E., Zimmerman, I.D., Albano, A.M., Deguzman, G.C. and Greenbaum, N.N. (1985). Dynamics of spontaneous neural activity in the simian motor cortex: the dimension of chaotic neurons. Phys. Lett. 110, 335–338.

Rosenblum, M.G. and Pikovsky, A.S. (2001). Detecting direction of coupling in interacting oscillators. Phys. Rev. E Nonlin. Soft. Matter Phys. 64, 045202.

Royet, J.P. and Plailly, J. (2004). Lateralization of olfactory processes. Chem. Senses 29, 731-745.

Rulkov, N.F., Sushchik, M.M., Tsimring, L.S. and Abarbanel, H.D. (1995). Generalized synchronization of chaos in directionally coupled chaotic systems. Phys. Rev. E Stat. Phys. Plasmas Fluids Relat. Interdiscip. Topics 51, 980–994.

Sato, A., Sato, Y. and Uchida, S. (2004). Activation of the intracerebral cholinergic nerve fibers originating in the basal forebrain increases regional cerebral blood flow in the rat's cortex and hippocampus. Neurosci. Lett. 361, 90-93.

Schliebs, R. and Arendt, T. (2006). The significance of the cholinergic system in the brain during aging and in Alzheimer's disease. J. Neural. Transm. 113, 1625-1644.

Skinner, J.E., Carpeggiani, C., Landisman, C.E. and Fulton, K.W. (1991). The correlation dimension of heartbeat intervals is reduced in conscious pigs by myocardial ischemia. Circ. Res. 68, 966-976.

Skinner, J.E., Molnar, M. and Tomberg, C. (1994). The point correlation dimension: performance with non-stationary surrogate data and noise. Integr. Physiol. Behav. Sci. 29, 217-234.

Skinner, J.E. and Molnar, M. (1999). Event-related dimensional reductions in the primary auditory cortex of the conscious cat are revealed by new techniques for enhancing the non-linear dimensional algorithms. Int. J. Psychophysiol. 34, 21-35.

Skinner, J.E., Pratt, C.M. and Vybiral, T. (1993). A reduction in the correlation dimension of heartbeat intervals precedes imminent ventricular fibrillation in human subjects. Am. Heart J. 125, 731-743.

Skinner, J.E., Nester, B.A. and Dalsey, W.C. (2000). Nonlinear dynamics of heart rate variability during experimental hemorrhage in ketamine-anesthetized rats. Am. J. Physiol. Heart Circ. Physiol. 279, 1669-1678.

Skinner, J.E., Yanculova, E.D., Yannopoulos, G. and Bountis, T. (2002). Nonlinear analysis of a Drosophila ECG time series. Dros. Inf. Serv. 85, 111-114.

Slooter, A.J., Vriens, E.M., Leijten, F.S., Spijkstra, J.J., Girbes, A.R., van Huffelen, A.C. and Stam, C.J. (2006). Seizure detection in adult ICU patients based on changes in EEG synchronization likelihood. Neurocrit. Care. 5, 186-192.

Smejkal, V., Druga, R. and Tintera, J. (2003). Olfactory activity in the human brain identified by fMRI. Bratisl. Lek. Listy. 104, 184-188.

Smirnov, D.A. and Bezruchko, B.P. (2003). Estimation of interaction strength and direction from short and noisy time series. Phys. Rev. E Stat. Nonlin. Soft. Matter. Phys. 68, 046209.

Smit, D.J., Stam, C.J., Posthuma, D., Boomsma, D.I. and de Geus, E.J. (2007). Heritability of "small-world" networks in the brain: A graph theoretical analysis of resting-state EEG functional connectivity. Hum. Brain Mapp. (Epub ahead of print)

Smit, L.S., Vermeulen, R.J., Fetter, W.P., Strijers, R.L. and Stam, C.J. (2004). Neonatal seizure monitoring using non-linear EEG analysis. Neuropediatrics. 35, 329-335.

Sowa, R., Chernihovskyi, A., Mormann, F. and Lehnertz, K. (2005). Estimating phase synchronization in dynamical systems using cellular nonlinear networks. Phys. Rev. E Stat. Nonlin. Soft Matter Phys. 71, 061926.

Stam, C.J. and van Dijk, B.W. (2002). Synchronization likelihood: an unbiased measure of generalzied synchronization in multivariate data sets. Physica D 163, 236-241.

Stam, C.J. (2005). Nonlinear dynamical analysis of EEG and MEG: review of an emerging field. Clin. Neurophysiol. 116, 2266-2301.

Stam, C.J. and de Bruin, E.A. (2004). Scale-free dynamics of global functional connectivity in the human brain. Hum. Brain Mapp. 22, 97-109.

Stam, C.J. and Pritchard, W.S. (1999). Dynamics underlying rhythmic and non-rhythmic variants of abnormal, waking delta activity. Int. J. Psychophysiol. 34, 5-20.

Stam, C.J., Breakspear, M., van Cappellen van Walsum, A.M. and van Dijk, B.W. (2003b). Nonlinear synchronization in EEG and whole-head MEG recordings of healthy subjects. Hum. Brain Mapp. 19, 63-78.

Stam, C.J., Jones, B.F., Nolte, G., Breakspear, M. and Scheltens, P. (2007). Small-world networks and functional connectivity in Alzheimer's disease. Cereb Cortex. 17, 92-99.

Stam, C.J., Montez, T., Jones, B.F., Rombouts, S.A., van der Made, Y., Pijnenburg, Y.A. and Scheltens, P. (2005). Disturbed fluctuations of resting state EEG synchronization in Alzheimer's disease. Clin. Neurophysiol. 116, 708-715.

Stam, C.J., Pijn, J.P.M. and Pritchard, W.S. (1998). Reliable detection of non-linearity in experimental time series with strong periodic components. Physica D 112, 361-380.

Stam, C.J., van Cappellen van Walsum, A.M., Micheloyannis, S. (2002). Variability of EEG synchronization during a working memory task in healthy subjects. Int. J. Psychophysiol. 46, 53-66.

Stam, C.J., van der Made, Y., Pijnenburg, Y.A. and Scheltens, P. (2003a). EEG synchronization in mild cognitive impairment and Alzheimer's disease. Acta Neurol. Scand. 108, 90-96.

Stam, C.J., van Woerkom, T.C. and Pritchard, W.S. (1996). Use of non-linear EEG measures to characterize EEG changes during mental activity. Electroencephalogr. Clin. Neurophysiol. 99, 214-224.

Takens, F. (1981). Detecting strange attractors in turbulence. Lecture in mathematics 366–381.

Takens, F. (1985). On the numerical determination of the dimension of an attractor. In Dynamical systems and bifurcations. Lecture notes in mathematics Springer Berlin/Heidelberg 1125, 99-106.

Theiler, J. (1986). Spurious dimension from correlation algorithms applied to limited time-series data. Phys. Rev. A 34, 2427–2432.

Tass, P., Rosenblum, M.G., Weule, J., Kurths, J., Pikovszki, A., Volkmann, J., Schnitzler, A. and Freund, H.J. (1998). Detection of n:m phase locking from noisy data: application to magnetoencephalography. Phys. Rev. Lett. 81, 3291-3294.

van der Hiele, K., Vein, A.A., Reijntjes, R.H., Westendorp, R.G., Bollen, E.L., van Buchem, M.A., van Dijk, J.G., Middelkoop, H.A. (2007). EEG correlates in the spectrum of cognitive decline. Clin. Neurophysiol. 118, 1931-1939.

Van Putten, M.J.A.M. (2003a). Proposed link rates in the human brain. J. Neurosci. Methods 127, 1-10.

Van Putten, M.J.A.M. (2003b). Nearest Neighbor phase synchronization as a measure to detect seizure activity from scalp EEG recordings. J. Clin. Neurophysiol. 20, 320-325.

Vybiral, T. and Skinner, J.E. (1993). The point correlation dimension of RR-intervals predicts sudden cardiac death among high-risk patients. In:Comput. in Cardiol. IEEE Computer Society Press, Los Alamitos 257-260.

Wojcik, D., Nowak, A. and Kus, M. (2001). Dimension of interaction dynamics. Phys. Rev. E 63, 1-15.